UNIVERSITY OF BEIRA INTERIOR
Sciences

Development of new therapeutic strategies for siRNA delivery

Patrícia Alexandra Nunes Pereira

Thesis for the obtention of a Master degree in

Biochemistry

(2nd Cicle of Studies)

Supervised: Prof. Doctor Fani Sousa and Prof. Doctor Ana Figueiras

Covilhã, June 2011

"Whether or not your efforts are smiled upon by fate,

what really matters in the end is to be able to say,

I did what I was able to"

Louis Pasteur

To my greatest loves,

My Parents…

Acknowledgments

My deepest gratitude is addressed to Professor Doctor Fani Sousa and Professor Doctor Ana Figueiras, not only for the guidance of this work, but also for the trust placed on me. I really appreciate all the dedication, availability and companionship throughout this year, the scientific expertise, as well as the criticisms and suggestions made during the guidance of the work.

To Professor Doctor João Queiroz from University of Beira Interior, I would like to express my sincere gratitude for his contribution and availability in the development of this research project.

I would also like to express my gratitude to all the people at the Health Sciences Research Centre at University of Beira Interior, especially to the Biotechnology and Biomolecular Sciences group for all their help, with a special recognition to Rita Martins and Filomena Silva for their support and friendship. Between a coffee and a laugh, these people were conspicuous by their unspeakable patience and willingness that contributed for this work to move forward.

I am deeply grateful to Vítor Gaspar, Ângela Sousa, Augusto Pedro and Ana Martinho for the time spent with me and for the enthusiastic way how they shared their knowledge.

I would also like to acknowledge Professor Doctor Alberto Canelas and Master Andreia Jorge from the Department of Chemistry, University of Coimbra, for the cordial way how they received me in their lab, for their vast knowledge and for all the teaching and scientific discussions during my brief but profitable stay in Coimbra.

I would also like to thank Eng. Ana Paula from the Optics Centre at the University of Beira Interior for all her help with the scanning electron microscopy experiments, and to Professor Doctor Graça Rasteiro from the Faculty of Engineering at the University of Coimbra for her kindness in allowing the use of the zetasizer equipment.

To Sofia and Margarida from CICS-UBI, for all the friendliness and availability.

To my family, especially my aunt Eduarda and my uncle Custódio, for always remembering me, despite my long absence from the family.

Finally, I will be eternally grateful to my parents for all their sacrifices, patience and love. I love you both.

Resumo

A importância do RNA em numerosos processos biológicos tem aumentado substancialmente nos últimos anos. Os RNAs de baixo peso molecular (sRNAs) são cada vez mais reconhecidos como moléculas reguladoras que desempenham papéis cruciais em todos os organismos. Devido à sua especificidade e eficácia, os sRNAs podem ser considerados promissores como agentes terapêuticos, nomeadamente na terapia baseada em RNA de interferência. Estas estratégias geralmente são baseadas na utilização de siRNA sintético. Embora a síntese de siRNA possa ser muito eficiente, verifica-se normalmente a presença de oligonucleótidos contaminantes, o que desencadeia a necessidade do desenvolvimento de novos processos de produção de siRNA com elevado grau de pureza, adequado para uso em terapia.

A bactéria *Rhodovulum sulfidophilum* tem a capacidade de secretar sRNA, existindo assim a possibilidade do uso deste microrganismo para a obtenção de sRNA recombinante, com elevada aplicabilidade terapêutica. No entanto, o sucesso das terapias baseadas em RNA depende também da capacidade de entrega do sRNA terapêutico, de forma selectiva e eficiente, aos órgãos-alvo, com a mínima toxicidade. Para este efeito, foram formuladas nanopartículas e outros veículos de entrega com elevada capacidade de transfecção e que possuem características ideais para a libertação do material genético.

A fim de optimizar a produção de sRNAs extracelulares usando a bactéria *Rhodovulum sulfidophilum* DSM 1374 foi estudada a influência da temperatura e concentração de NaCl no crescimento e na produção de sRNA extracelulares. Os ensaios realizados demonstraram que o crescimento em aerobiose, na ausência de luz, a 30 ºC, em meio NB suplementado com 3 % de NaCl, conduziu a uma produção máxima 197 ± 0,55 µg/mL de sRNAs extracelulares.

Tendo em vista o aperfeiçoamento das terapias baseadas no RNAi foram desenvolvidos vectores não virais para a entrega de siRNA usando polímeros comerciais, tais como polietilimina, quitosano e poli(alilamina). Os resultados obtidos demonstraram que as propriedades estruturais (tamanho, potencial zeta e morfologia) das nanopartículas são fortemente dependentes do peso molecular, da densidade de carga e estrutura do policatião. Para além destas observações, verificou-se que o quociente entre os grupos amina do policatião e os grupos fosfato do RNA (N/P rácio) também afecta a formulação das nanopartículas. Por conseguinte, quaisquer alterações nestes parâmetros irão influenciar a eficiência de encapsulação, bem como a protecção e estabilidade do sRNA. A conjugação destas tecnologias inovadoras oferece um ponto de partida para o futuro desenvolvimento de aplicações baseadas em siRNA com relevância terapêutica.

Palavras-chave

Terapia baseada em RNA, siRNA, *Rhodovulum sulfidophilum* DSM 1374, Nanopartículas, Poliplexos

Abstract

The importance of RNA in numerous biological processes has increased substantially over recent years. Small RNAs (sRNAs) are increasingly recognized as crucial regulatory molecules in all organisms and the specificity and potency of small RNAs suggest that they might be promising as therapeutic agents, namely in interference RNA strategies. These strategies generally rely on the use of synthetic siRNA. Although the synthesis of siRNA can be very efficient, the oligonucleotides typically present contaminants, which leads to the need for the development of new processes for the production of highly purified and clinically suitable siRNA oligonucleotides for use in therapy. *Rhodovulum sulfidophilum* have the ability to produce active extracellular sRNA; therefore, the potential use of this organism to obtain functional recombinant sRNA with large therapeutic applicability is eminent. However, the success of sRNA therapies depends upon the ability to selectively and efficiently deliver therapeutic sRNA to target organ with minimal toxicity. For this purpose, novel nanodevices and vehicles have been formulated with materials that possess ideal intrinsic transfection and unpacking characteristics.

In order to optimize the production of *Rhodovulum sulfidophilum* DSM 1374 extracellular sRNAs, the influence of temperature and NaCl concentration on the specific growth rate and in extracellular sRNA production were evaluated. The experiments performed showed that the aerobic cultivation in the dark, with nutrient broth medium containing 3 % NaCl at 30 ºC, conducted to a maximum production of extracellular sRNAs yielding 197 ± 0.55 µg/mL. For the improvement of the biological effect in RNAi-based therapies, the design and synthesis of optimal non-viral vectors for sRNA delivery, using commercial polymers, such as Polyethylenimine, Chitosan and Poly(allylamine) were performed. The results obtained showed that the structural and physicochemical properties (size, zeta potential and morphology) of the nanoparticles are strongly dependent on polycation molecular weight, charge density and structure, and also on the formulation ratio of amine to phosphate groups present in the RNA (N/P ratio) and, ultimately, alterations in these parameters influence the association efficiency and stability of sRNA. Overall, the implementation of this cutting-edge approach provides the basis for the future development of effective sRNA-based gene therapy applications.

Keywords

RNA therapeutic, siRNA, *Rhodovulum sulfidophilum* DSM 1374, Nanoparticles, Polyplexes

Table of Contents

List of Figure

Page

Chapter I - Introduction

Chapter II – Materials and Methods

Chapter III – Results and Discussion

List of Tables

Page

Chapter I - Introduction

Chapter III – Results and Discussion

List of Acronyms

Ago2	Argonaute 2
BHI	Brain Heart Infusion
Bp	Base pair(s)
CD	Circular dichroism
CS	Chitosan
DEPC	Diethyl pyrocarbonate
DD	Deacetylation degree
DNA	Deoxyribonucleic acid
dsRNA(s)	Double-stranded RNA(s)
E. coli	*Escherichia coli*
EE	Encapsulation efficiency
FBS	Fetal bovine serum
gDNA	Genomic DNA
h	Hour
MHI	Mueller Hinton
min	Minute
miRNA(s)	microRNA(s)
mRNA	messenger RNA
NaCl	Sodium chloride
NB	Nutrient Broth
nm	Nanometer
nt	Nucleotide
OD_{600}	Optical density at 600 nm
ODNs	Oligonucleotides
PAA	Poly(allyamine)
PEI	Polyethylenimine
P.I.	Polydispersion index
RISC	RNA-induced silencing complex
RNA	Ribonucleic acid
RNAi	RNA interference
RNase(s)	Ribonuclease(s)
rRNA(s)	Ribosomal RNA(s)
rpm	Revolutions per minute
R. sulfidophilum	*Rhodovulum sulfidophilum*

s	Second
shRNA	Short hairpin RNAs
siRNA	Small interfering RNA
sRNA	Small RNA
tRNA(s)	Transfer RNA(s)
TS	Tryptone Soya
UV	Ultraviolet
V	Volt

CHAPTER I

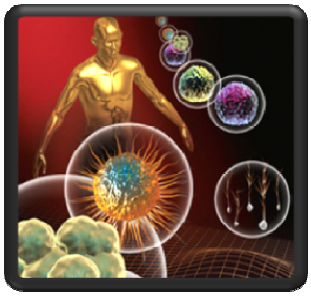

Introduction

Gene therapy has gained significant attention over the past two decades as a promising approach due to its high potential as a future therapeutic strategy for clinical applications, not only for the treatment of diseases caused by genetic defects, but also in the development of strategies for treatment and prevention of a wide range of acquired disorders such as severe combined immunodeficiency, cystic fibrosis, cardiovascular disease, rheumatoid arthritis, viral infections and neurodegenerative diseases, as well as an alternative method to traditional chemotherapy for cancer treatment [1-3]. Therefore, gene therapy can be defined as the transfer of genetic materials to specific cells in order to have a therapeutic effect, by replacing defective genes, substituting missing genes, silencing unwanted gene expression or producing bioactive agents [4-6]. Gene therapy involves delivering polynucleotides such as DNA, RNA, anti-sense oligonucleotides and small interfering RNA, either locally or systemically.

Presently, short interfering RNA (siRNA) is the most commonly employed tool for gene silencing since the recent advances in molecular biology have shown that gene expression can be silenced in a highly specific manner through the target mRNA degradation [7]. In fact, the silencing of specific intracellular expression mechanisms is a strategy that encloses an enormous therapeutic potential that could change the course of the currently applied treatments in several severe and chronic pathologies [8]. Generally, siRNA-based gene therapy applications rely on the use of synthetic siRNA. However, issues associated with the presence of contaminants in these synthesized formulations still restrict the implementation of these oligonucleotides onto pre-clinical and clinical applications. Therefore, the requirement for the production of highly purified and clinically suitable siRNA oligonucleotides arises as one of the most important challenge in the development of therapeutic strategies based on this technology. Nowadays with the recent advance of nanomedicine, different and innovative mechanisms are being developed in order to enhance the production, purification and especially the siRNA delivery, revolutionizing the way that genetic material is transported towards and into the cell [9]. Therefore, the use of polycationic nanoparticles is a method that can be used to improve the therapeutic potential of siRNA.

Hence, the purpose of this thesis is to develop and implement a new strategy for extracellular sRNA biosynthesis using the bacterium *Rhodovulum sulfidophilum* DSM 1374, resulting in the

improvement of sRNA production and quality. The recovery is based on a single step of isopropanol precipitation, in order to accomplish a less time-consuming and economics procedure. In addition, the development and characterization of a siRNA delivery vehicle is also envisioned, since the delivery of these oligonucleotides into the cytoplasmic compartment, the location where their function is exerted, is usually a critical barrier to an efficient therapeutic response.

Briefly, the work described may be divided in three main stages purposes:

1) The first comprises the evaluation of the influence of variables such as NaCl concentration, pH and temperature in *R. sulfidophilum* DSM 1374 growth and its sRNA extracellular production;

2) The second stage consists on the development of the nanocarrier system with differing N/P ratios between the polycation, as Linear-Polyethylenimine, Branched-Polyethylenimine, Chitosan (Low and Medium Molecular Weight), Poly(allyamine) and a *Escherichia coli* bacterial sRNA, as a model;

3) The final research topic is based on the assessment of biophysical and structural characteristics (such as size, zeta potential, morphology and complex stability) of the polymer-sRNA complexes, in order to achieve a successful delivery system for sRNA.

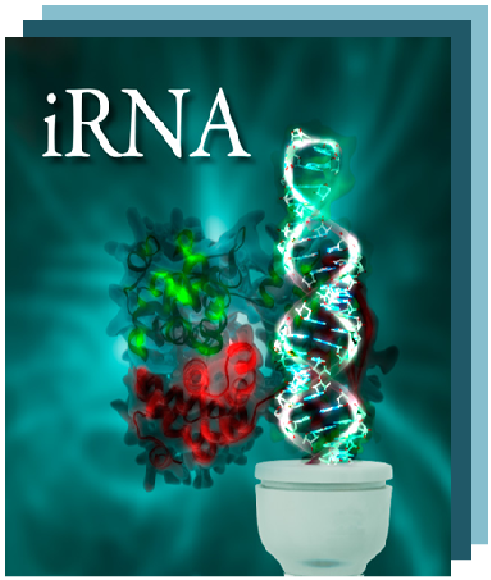

Section I

Interference RNA

Research's increasing awareness of RNA role in a variety of cell processes and in the progression of some diseases makes the discovery of new RNA targets an emerging field for therapeutic treatments. RNAs are increasingly recognized as crucial regulatory molecules in all organisms and the specificity and potency of small RNAs suggest that they might be promising as therapeutic agents, namely in interference RNA (RNAi) strategies [10, 11]. In 1990, Richard Jorgensen's plant biology group was the first to note the effects of administration of specific RNA molecules on gene expression [12]. In their landmark paper, Fire and Mello showed that sequence-specific gene knockdown was possible by microinjection of synthetic double-stranded RNA (dsRNA) in the nematode *Caenorhabditis elegans* [13]. Furthermore, they showed that the use of dsRNA was over 10 times more potent than either sense or antisense RNA alone, also that gene silencing was possible on administration of only a few molecules of dsRNA and that this effect may be passed on to first-generation progeny [13]. The term 'RNA interference' was applied to their findings and they were awarded the Nobel Prize for Medicine in October 2006.

Subsection I

siRNA applications in nanomedicine

RNA interference is a well-conserved, ubiquitous, endogenous mechanism in higher eukaryotic cells that uses small noncoding RNAs to eliminate harmful or unwanted genes, through the specific destruction of their mRNA molecules [14]. In addition, RNAi has also become a method of choice for key steps in the development of therapeutic agents, from target discovery and validation to the analysis of the mechanisms of action of small molecules. The highly efficient and specific gene silencing by RNAi is applicable to all classes of molecular RNA as a powerful new therapeutic agent that reduces or eliminates undesirable small molecules and proteins targets [15]. Therefore, RNAi has attracted a great deal of attention on, as a powerful and potent therapeutic strategy to downregulate target gene expression in clinical applications.

The RNAi mechanism can be mediated in several ways, including double stranded small interfering RNAs (siRNAs) cellularly delivered as synthetic duplexes, short hairpin RNAs (shRNAs) and microRNA (miRNA) [16, 17]. Nevertheless, siRNA is the most commonly used one for RNAi in therapeutic applications (Table 1).

Table 1 – Small noncoding RNAs use in RNAi technology (Adapted from [18]).

Gene silencing mechanism	*Description*	*Stability in serum*
RNAi		
siRNA	21–25 nt, double-stranded, endogenous or exogenous, natural defense against viruses and transposons, regulate mRNA degradation posttranscriptionally with perfectly matched sequences	Several minutes to 1 h
Small interfering RNA		
shRNA	Similar to ds-siRNA with a 4–9 nt loop at one end, processed by Dicer to produce siRNA, transcribed by RNA polymerase III	More durable than siRNA
Short hairpin RNA		
miRNA	20–24 nt, endogenous, transcribed by RNA polymerase II, regulate mRNA degradation or translation inhibition posttranscriptionally with partial mismatched sequences	----

RNAi regulates gene expression in various cellular pathways through siRNA, endogenously produced or exogenously introduced, which become incorporated with the RNA-induced silencing complex (RISC) leading to the cleavage and degradation of the complementary target mRNA (Figure 1) [19]. Specifically, when the long dsRNA (> 30 nt) is inside the cell, the process of RNAi begins with the enzymatic degradation of the dsRNA by an endoribonuclease, of the RNase III family known as Dicer, into short RNA duplexes of 21 nucleotides, termed siRNA. These siRNAs have a characteristic sequence of 19 nucleotides of complementary with 5'-terminal phosphate groups and 2 nucleotides 3' overhangs, termed siRNA (Figure 1) [15, 20].

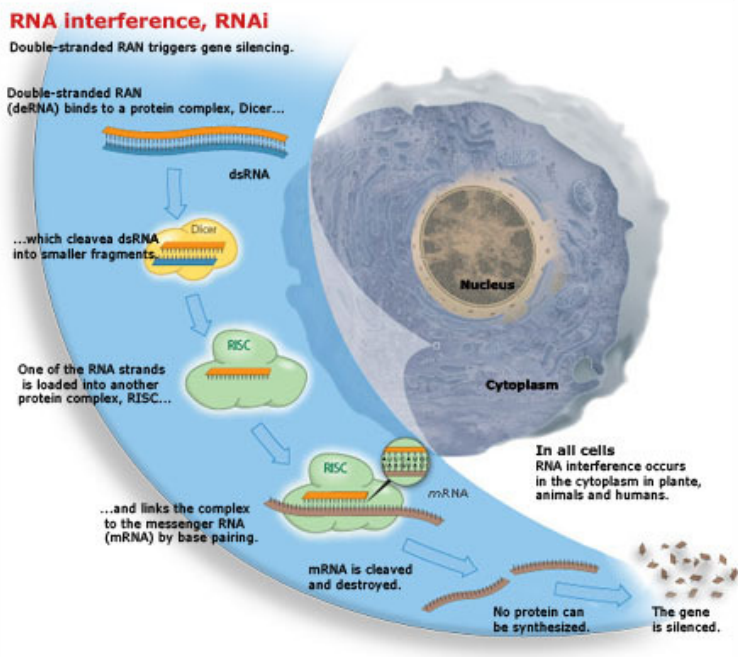

Figure 1 - Mechanisms of small RNA interference (siRNA). Long dsRNA are processed by Dicer into 21-23-nt siRNA duplexes. Processed siRNAs assemble with cellular proteins to form RISC. During RISC assembly, one strand is eliminated, while the other strand (guide) induces the activation of RISC, which eventually triggers the sequence-specific mRNA degradation (in case of total complementarity) (Adapted from [21]).

Dicer acts in concert with a dsRNA-binding protein HIV transactivating response RNA-binding protein (TRBP) in mammalian cells which binds to the more thermodynamically stable end of the duplexed RNA (Figure 2). This interaction helps to determine the orientation of siRNA loading onto Argonaute 2 (Ago2), the catalytic core of the RNA-induced silencing complex (RISC) [22]. In a second stage, siRNAs reach the cytosol of cells, and binds to a multiprotein complex (nucleases and other proteins) termed RISC. After incorporation into RISC, the siRNA is then unwound by the enzyme Ago2 and the sense strand is cleaved and released, leaving the guide strand to direct the activated RISC to the complementary sequence in the target mRNA. This leads to the silencing of gene expression (Figure 2) [15, 23, 24].

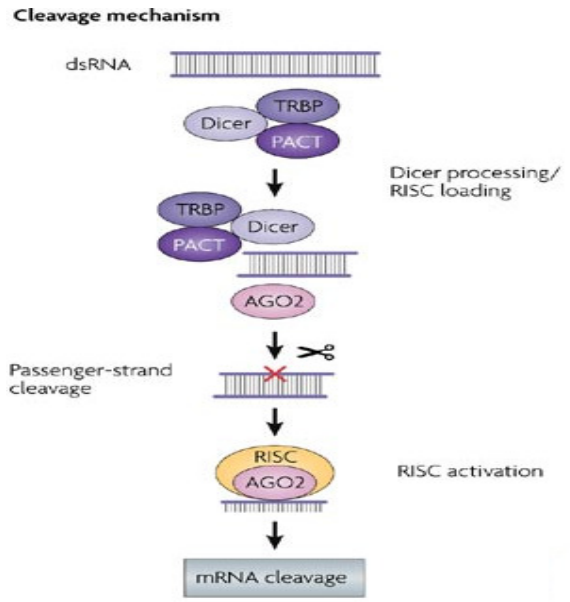

Figure 2 - RISC loading and activation. Double-stranded RNAs (dsRNAs) are processed by a complex comprising Dicer, TAR RNA-binding protein (TRBP) and protein activator of protein kinase PKR (PACT), facilitating loading of the small interfering RNA (siRNA) duplex into Argonaute 2 (AGO2) and RNA-induced silencing complex (RISC). When the RNA duplex loaded into RISC has perfect sequence complementarity, AGO2 cleaves the passenger strand so that active RISC is produced that contains the guide strand, which is complementary to the target sequence (Adapted from [24]).

Because an activated RISC is capable of repeatedly cleaving mRNA, this process effectively promotes gene silencing over a significant period of several days [23]. The discovery by Tuschl and colleagues (2001) that the introduction of chemically synthesized siRNAs into mammalian cells efficiently induced sequence-specific inhibition of gene expression propelled RNAi-based silencing approaches to the forefront of modern molecular biological research [15]. In addition, it became evident that harnessing these endogenous pathways could prove to be an effective mechanism for the targeted silencing of disease-causing genes. Thus, endogenous and exogenous siRNA have been found to suppress the *in vitro* gene expression in mammalian cells. Therefore, siRNA has become an indispensable tool for studying gene function in mammalian cells and the sequence specific interaction on the mRNA level holds great promise for a vast variety of gene-specific therapeutics [15]. The advantages of siRNA as a potential therapeutic agent are due to its naturally occurring conserved phenomenon with high specificity, and there is no limitation for its target gene/mRNA.

In addition, the success of nucleic acid therapies relies on the ability to efficiently deliver the appropriate therapeutic material into the target tissue or cells with the least toxicity and without inducing an immune response. Briefly, the use of siRNAs as therapeutics begins with (1) the design of siRNAs which target the mRNA of a protein that causes disease or whose

downregulation results in tissue formation; (2) the incorporation of siRNAs into a delivery vehicle that can efficiently deliver the siRNAs *in vivo*, and (3) the delivery of the siRNA/vehicle complex to the desired tissue/site, where the siRNA can effectively silence the gene and achieve the desired therapeutic response (Figure 3) [18]. So, if all the previous steps described have been completed, interference RNA provides a specific and efficient way to silence gene expression, being an attractive tool for genetic research and drug target validation, and may provide new therapeutic options for nondruggable targets.

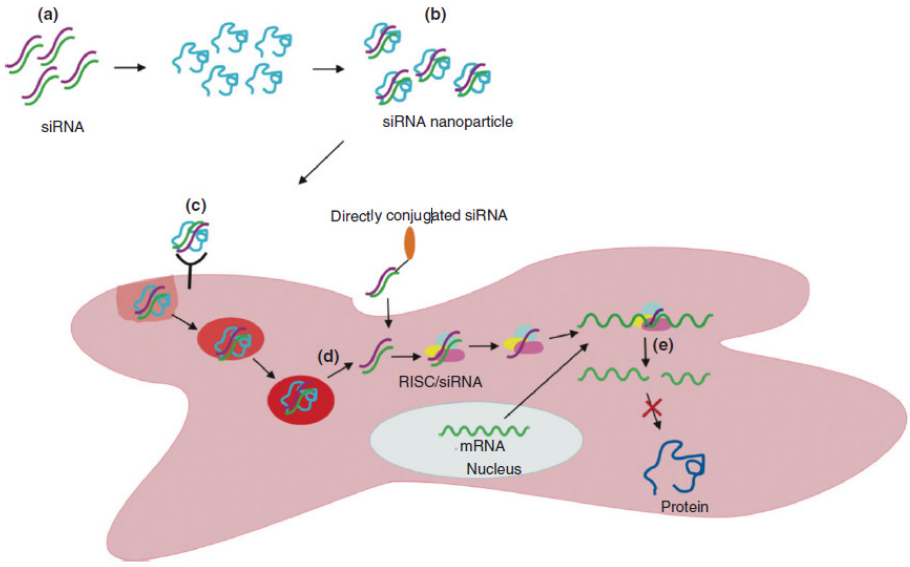

Figure 3 – Scheme representation of the limitations to siRNA delivery and the siRNA-induced RNAi pathway. Limitations to siRNA delivery include: (A) siRNA stability, (B) siRNA nanoparticle stability, (C) siRNA or siRNA nanoparticle targeting and internalization, (D) siRNA endosomal escape, and (E) siRNA off-target effects (Adapted from [18]).

Subsection II

In vivo delivery siRNA

The application of siRNAs as potential therapeutic silencing agents requires the development of vehicles that can effectively direct siRNAs to the cytoplasm of the appropriate target cells in clinically relevant doses. To be effective, these vehicles must be optimized at all stages of the delivery process, from target-cell recognition to uptake into RISC and mRNA cleavage. At the moment, the successful clinical use of siRNA is limited due to some problems, such as: (1)

rapid enzymatic degradation of siRNA by ubiquitous nucleases resulting in a short half-life in the blood; (2) poor cellular uptake when delivered in the aqueous solutions due to its negative charge; and (3) insufficient tissue bio-availability, particularly following systemic administration. These facts have stimulated the development of carrier system for gene delivery [25]. Table 2 summarizes the main limitations faced by siRNA through its delivery and internalization process and possible strategies to overcome the stated limitations extracellular and intracellular.

Table 2 – Extracellular and Intracellular limitations of RNAi using siRNA (Adapted from [18]).

Limitation	*Possible solution(s)*
Extracellular	
Degradation in serum	• Chemical modification with PEG, etc. • Peptide/polymer/lipid complexation • Nanoparticle encapsulation
Targeting to specific cells	• Vector modification with targeting ligands
Internalization	• Peptide/polymer/lipid complexation for charge neutralization • Conjugation or complexation with cell penetrating peptides • Ligand modification for receptor-mediated endocytosis
Intracellular	
Endosomal escape	• Conjugation or complexation with fusogenic peptides • Acid-responsive polymers/lipid complexation
mRNA targeting	• Chemical modification of siRNA

As a result of these limitations, native delivery of siRNA to the cells is not effective. Although various chemical modifications of siRNA can be used to overcome these problems, these modifications are also associated with certain disadvantages such as a decrease on mRNA hybridization, higher cytotoxicity and increased unspecific effects. Therefore, effective systems which can protect and efficiently transport siRNA to the cytoplasm of the target cells are needed to exploit the promising potential applications offered by successful delivery of siRNA.

These delivery approaches aim to: (1) increase the retention time of the siRNAs in the circulatory system by reducing the rate of renal clearance; (2) protect the siRNAs from serum nucleases; (3) ensure effective biodistribution; (4) facilitate targeting to and uptake of the siRNAs into the target cells; and (5) promote trafficking to the cytoplasm and uptake into RISC. A variety of approaches have been developed that promote siRNA delivery *in vivo*, including cationic nanoparticles [26], lipids and liposomes [27, 28], antibody (Ab)-fusion molecules [Ab-protamine [29]], as well as cholesterol [30] and aptamer-conjugated siRNAs [31].

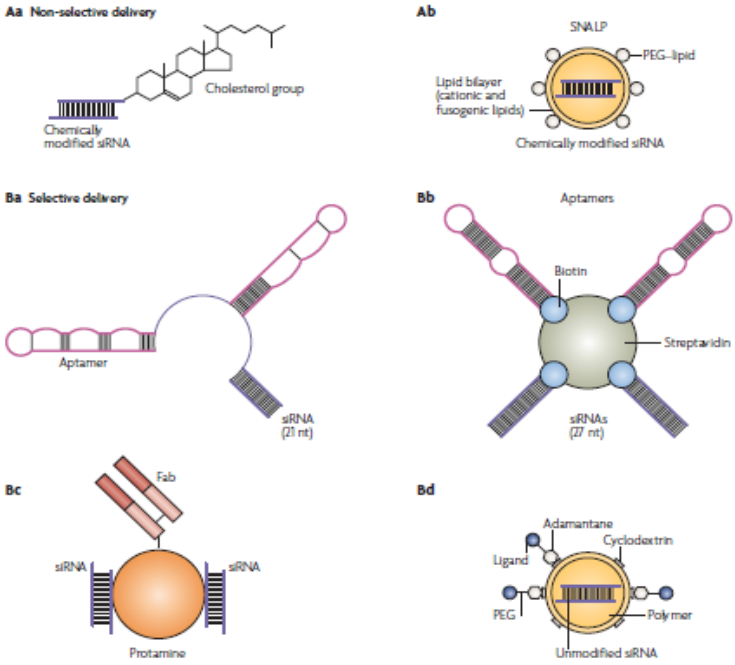

Figure 4 – Delivery of small interfering RNAs (Adapted from [24]).

To date, the mentioned strategies have been devised to trigger the RNAi pathway, each of which is adapted and optimized for different cell systems. However, this approach presents some bottlenecks regarding the sustained expression of the vector and its delivery into the intracellular environment. In fact, it is important to underline that often the concept of gene therapy is mostly referred as gene delivery, since the entry of the vector in the cell is the key factor that as hindered the translation of this technique into a clinical application.

Subsection III

Intracellular trafficking of siRNA

1. Cellular uptake

Internalization into the target cell constitutes the first step in the cellular gene transfection process. The plasma membrane represents a relevant barrier for siRNA uptake, since it is negatively charged, owing to their content of glycoproteins, glycerolphosphates and sulphated proteoglycans [32]. Despite their small size, the hydrophilicity and negative charge of siRNA molecules prevent them from readily crossing biological membranes. Electrostatic repulsions between the cell surface and RNA are responsible for endocytosis of a small amount of free RNA by cells. In the case of using synthetic delivery vectors, since they are formulated with excess of positive charge, these condense the RNA and interact associated with the cell surface through charge interaction [33]. This association is essentially mediated by binding between the positive charge of these nanoparticles and negatively charged cell membranes [32]. As figure 5 shows there are a multitude of entering pathways, although the predominant way that nanocarriers use to enter in the intracellular compartment seems to be the easier, i.e. the one that relies on non-specific endocytosis, followed by the clathrin-coated mechanism (Figure 5) [33, 34]. Nonetheless, it is important to state that the contribution of each pathway to the internalization of the carriers is not yet defined due to their different constitution. This binding process leads to endocytosis of particles <200 nm in diameter. In fact, among the factors that may set of the entry into the cell trough one mechanism in detriment of other are the size of the carriers and their surface charge [32]. Upon binding to the cell, these cell-type-specific delivery vehicles and the associated siRNAs are taken up by receptor mediated endocytosis and deposited into endosomes.

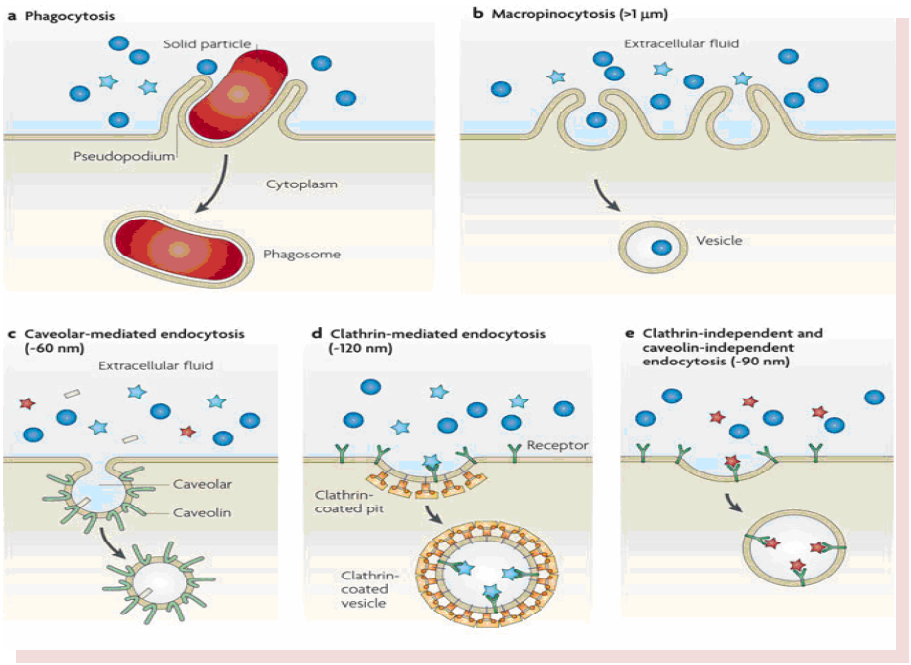

Figure 5 – Modes of cellular internalization of nanoparticles and respective size limitations. Internalization of large particles is facilitated by phagocytosis (a). Nonspecific internalization of smaller particles (>1 µm) can occur through macropinocytosis (b). Smaller nanoparticles can be internalized through several pathways, including caveolar-mediated endocytosis (c), clathrin-mediated endocytosis (d) and clathrin-independent and caveolin-independent endocytosis (e), with each being subject to slightly different size constraints. Nanoparticles are represented by blue circles (> 1 µm), blue stars (about 120 nm), red stars (about 90 nm) and yellow rods (about 60 nm) (Adapted from [35]).

2. Endosomal escape

Cellular internalization of nucleic acid-containing vectors occurs mostly by endocytosis. As a result, these vectors are included within intracellular endosomal vesicles, which present itself as a major drawback to efficient transfection. Actually, if the nanoparticle carrier stays for indeterminate time in the vesicle it will most likely be degraded by lyzosomes, and the delivery of the genetic material is not efficiently concluded (Figure 6) [36].

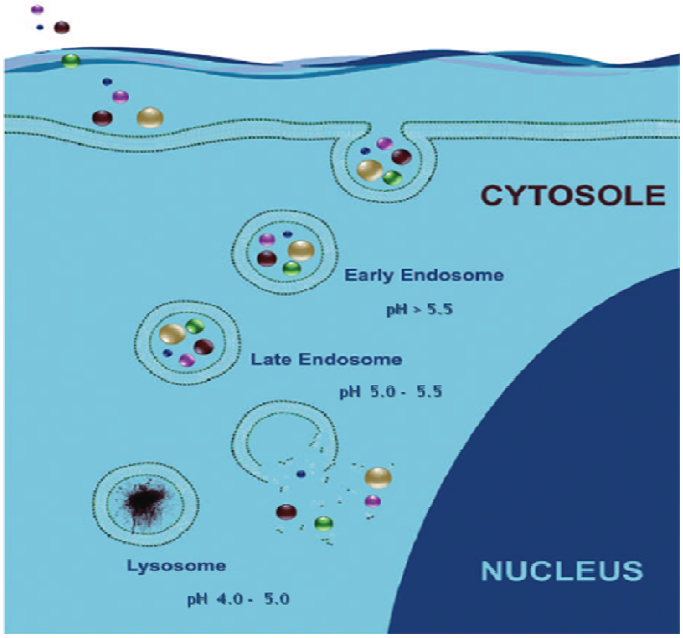

Figure 6 – An artistic representation depicting the internalization of therapeutics into the cell through endocytosis and subsequent endosomal escape. Early endosomes consist of the vesicles containing the therapeutics coming from the cell surface. Late endosomes which are thought to mediate a final set of sorting events prior to interaction with lyzosomes receive the internalized materials from early endosomes. Lyzosomes as the last parts of the endocytic pathway contain the hydrolytic enzymes which digest the contents of the late endosomes. Therefore, the endosomal release of the therapeutics is necessary before lyzosome mediated digestion of the therapeutics (Adapted from [37]).

These early endosomes subsequently fuse with sorting endosomes, which in turn transfer their contents to the late endosomes. Late endosomal vesicles contain vacuolar ATPase proton pumps, which lower pH from 7.4 to ~ 5.0, so they are acidified. In these late stages, the endosomal content is then relocated to the lyzosomes (the main degradative compartment of the cell) that also contain a low pH (pH ~ 4.5) environment and a high concentration of nucleases that may promote the degradation of the siRNAs (Figure 6) [38]. Thus, to avoid lysosomal degradation, siRNAs (free or complexed with the carrier) must escape from the endosome into the cytosol, where they can interact with the RNAi machinery. The cellular endosome is a major barrier for efficient siRNA delivery [39].

To accomplish this, polymeric systems typically utilize tertiary amine functionalities to cause endosomal rupture by increasing the osmotic pressure during acidification. Among various cationic polymers, polyethylenimine (PEI) possesses inherent endosomolytic activity and has potential to be protonated at physiological pH. These polycations are believed to escape the endosomes via the proton sponge mechanisms as depicted in Figure 7.

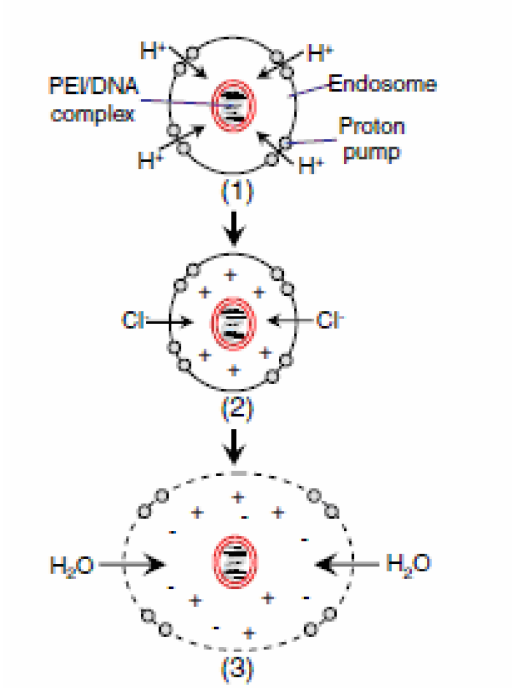

Figure 7 - Proton sponge mechanism. The polyplex exacerbates proton accumulation in the endosome (1), inducing passive chloride influx (2), and causing osmotic swelling and endosomal rupture (3) (Adapted from [38]).

Briefly, the buffering capacity of the polymers prevents the acidification of the endosomes, which causes more and more protons to be pumped inside the endosomes, accompanied with an influx of Chloride ions. Thus, the proton sponge effect is a consequence of the increase in osmotic pressure with accumulation of water in the endosomes [38]. This, in combination with osmotic swelling (due to positive charge of the nanocarrier systems) finally causes endosomes to rupture with release of polyplexes in the cytosol of the cell. The "proton sponge" is a crucial characteristic that determines the choice of materials for their synthesis, as it shall be seen further ahead.

3. Delivery in the cytoplasm

The last and the most important step to intracellular trafficking of siRNA is the disassembly of the nucleic acids from the vector. To fulfill this requirement, the delivery system must bind RNA tightly enough to protect it from nucleases mediated degradation, but at the same time it should be able to release the RNA, not affecting its activity. Although, the question about when is the best moment for this event to take place arises [40]. A limiting factor in this step

is the presence of cytosolic nucleases, which degrade RNA with a half-life of 50–90 min [41]. Consequently, a delivery system must protect RNA from degradation and improve its transport through the cell. The mechanism involves displacement of nucleic acids by intracellular polyanions, which is essentially influenced by the chemical structure of the delivery vehicle. Therefore, it requires careful designing of the chemical vectors in such a way that on transition from extracellular to intracellular environment, the binding capability/strength of the vector must decrease, resulting in the release of the RNA [38, 40].

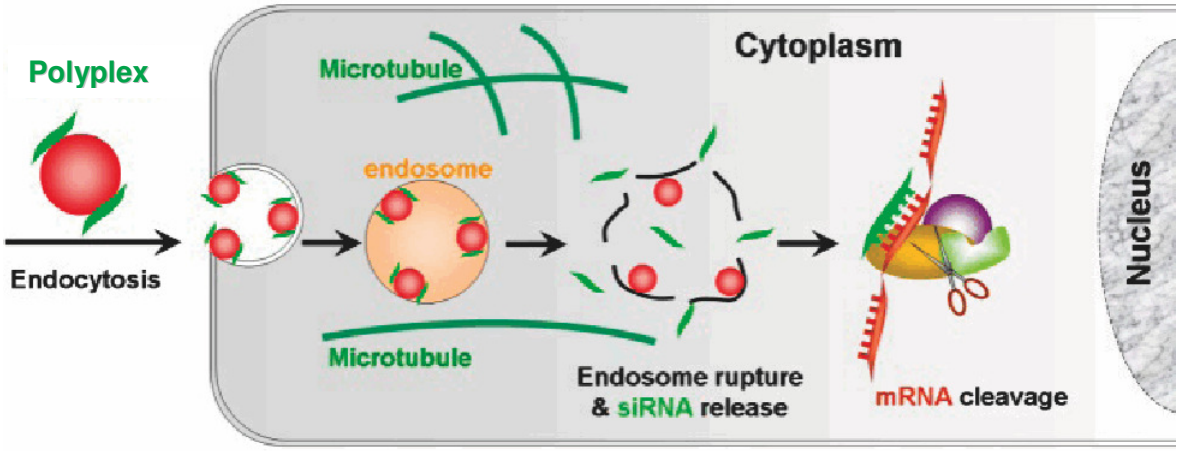

Figure 8- Scheme representation of siRNA delivery (Adapted from [42]).

Section II

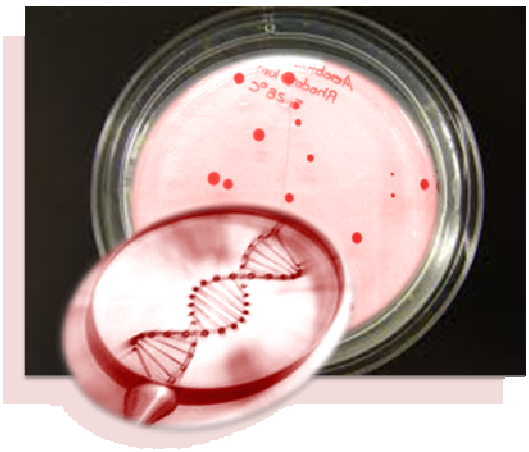

sRNA production in Rhodovulum sulfidophilum

As it was stated before, several research studies have shown that sRNAs are crucial regulatory molecules in microorganisms, plants and animals and, therefore, they are becoming promising target molecules due to their specificity as repressors of gene expression and potential as therapeutic tools for treating diseases. Therefore, the development of new sRNA production strategies is a requirement for its therapeutic application, since the current methods make use of *in vitro* transcription or chemical synthesis, which require expensive enzymes, synthetic DNA templates, or chemicals, making these processes time-consuming and labor-intensive. The methods implemented for the recombinant production and isolation of sRNAs uses as preferential hosts several bacteria such as *Escherichia coli* (*E. coli*), *Listeria monocytogenes* or *Clostridium spp*. Very recently, another bacterium was described as a potential RNA aptamers producer, the marine bacterium *Rhodovulum sulfidophilum* (*R. sulfidophilum*) DSM 1374 [43-45].

R. sulfidophilum (formerly *Rhodobacter sulfidophilus*) is a facultative phototrophic bacterium that can grow anaerobically in the presence of light or aerobically in the dark with a wide variety of organic compounds as electron donors and carbon sources [44].

Sunlight-exposed stagnant water in tidal and seawater pools in which sulfide is produced during rapid decomposition of organic matter provides growth conditions favorable for anoxygenic phototrophic bacteria. In such environments, these bacteria often occur in great numbers and are visible as pink, red, brown, or green blooms (Figure 9) [43].

Figure 9 – Photograph of the bacteria *R. sulfidophilum* DSM 1374 after 2 days of cultivation.

Within the species *sulfidophilum* of the genus *Rhodovulum* is recognized the strain PS88, isolated from colored blooms occurring in the coastal areas in Japan, and the commercial strains DSM 1374 and 2351.

However, most of the studies on the characterization of *R. sulfidophilum* are performed in strain PS88. In general, *R. sulfidophilum* PS88 is able to grow in the presence of sodium chloride (NaCl) concentrations ranging from 0 to 10 %, but the best conditions are described

to be an optimum NaCl concentration of 2 to 5 % and pH ranging from 5.0 to 9.0 [44]. In addition, the optimum temperature is described to be between 30 and 35 ºC, for the strain PS88 and DSM 1374 [43, 44]. Watanabe and co-workers (1998) have demonstrated that *R. sulfidophilum* PS88 has a self-flocculating ability, which is due to the active secretion of the extracellulary produced nucleic acids [46, 47]. The production of extracellular nucleic acids occurs simultaneously with cell growth. Thus, it seems unlikely that the release of extracellular nucleic acids is due to the usual cell autolysis in the post-stationary phase. Some active production mechanisms should exist. Another possibility is that a kind of programmed cell death might occur: partial cell death might be induced by a high level of cell density. In fact, such a mechanism has been found in *Streptococcus pneumonia* [48, 49]. The cell lysis of *S. pneumonia* is induced by an extracellular concentration of a secreted peptide pheromone called the competence stimulation peptide (CSP) [50] by a quorum sensing mechanism [51]. CSP also induces a competent state of this bacterium, and the extracellular nucleic acids produced are used for genetic transformation. The competent state of this bacterium is triggered when CSP reaches an extracellular concentration of 1–10 ng/mL, which corresponds to a population density of about 10^7 cells per mL [48]. Similar cell concentration (CSP concentration) induces the cell lysis of *S. pneumoniae*. It is possible that a similar mechanism occurs in *R. sulfidophilum*.

Furthermore, the studies already published with the commercial *R. sulfidophilum* DSM 2351 showed that the extracellular nucleic acids are a mixture of double-stranded DNAs and single-stranded RNAs, mainly nonaminoacylated fully mature transfer RNAs (tRNAs) and fragments of 16S and 23S ribosomal RNAs (rRNAs) [52-55]. The commercial DSM 1374 strain has only been studied by Suzuki et al. (2010) which reported the potential of this strain for the production of artificial RNA under anaerobic conditions. However, despite the interesting results obtained, bacterial growth and RNA production was rather complex [56].

The common fact of using *E. coli* as a recombinant host involves the cell lysis and extraction of nucleic acids, which can be a laborious and time-consuming procedure due to the number and complexity of the processing steps [57-59]. Therefore, the main advantage of using *R. sulfidophilum* as recombinant host over the others is the production of nucleic acids into the culture medium [60], that represents a significant benefit to the isolation process. Moreover, there are strong evidences that the *R. sulfidophilum* does not produce any detectable RNases in the culture medium [54, 56], while *E. coli* expresses several endonucleases leading to nucleic acid degradation. Thus, this fact constitutes an additional advantage since RNA is an instable molecule due to its susceptibility to endo- and exonucleases (RNases) mediated degradation. It becomes therefore clear that the production of RNA in *R. sulfidophilum* may provide a valuable alternative to current RNA production approaches. In the point of view of the scalable and efficient biotechnological process the fast and single-step isolation of biologically competent and chemically stable sRNAs is thus a central procedure to explore their potential as therapeutics agents

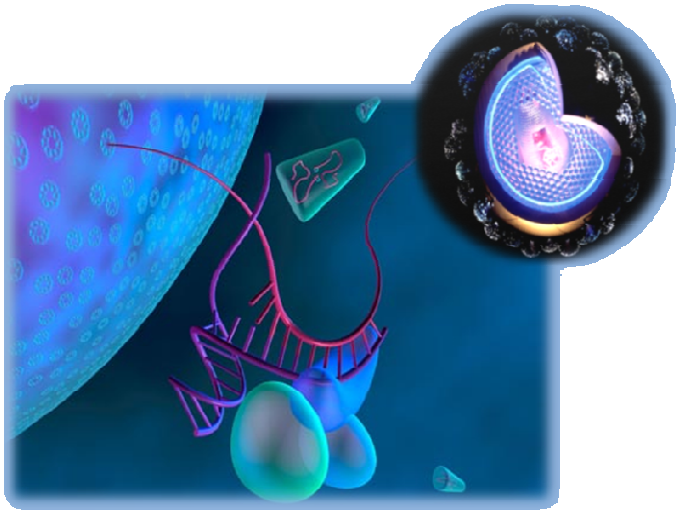

Section III

Non-viral gene delivery vectors

The key issue of designing new non-viral gene vectors is to enhance the gene delivery capability as well as to improve the biocompatibility. In the past few decades, the majority of non-viral gene delivery systems comprise a wide number of polycations including cationic lipossomes, polyethylenimine (PEI), poly-L-Lysine, polyamidoamine dendrimers, polyarginine and chitosan, among others [61, 62]. There are many other polycations with more complex structures such as branched polycations, block copolymers, grafted polymers, and so on, that induce effective RNA compaction. These polycations are a promising alternative for compacting RNA for systemic delivery because of their low cytotoxicity, low immunogenicity, high stability, biocompatibility, and unrestricted gene materials size, which make these compounds increasingly attractive for gene therapy [63-65]. Moreover, non-viral vectors present high manipulability, relatively low production cost and high flexibility, allowing to design carriers with well-defined structural and chemical properties on a large scale [2]. Briefly, polycationic polymers have been preferred over other systems due to their ease preparation, purification and chemical modification along with the long shelf life [65]. Nanoparticles applied as drug delivery systems are submicron particles (3-200 nm), devices, or systems that can be made using a variety of materials including polymers (nanospheres, micelles, or dendrimers), lipids (liposomes) and nanocapsules, which can be defined as solid colloids as shown in Figure 10 [66].

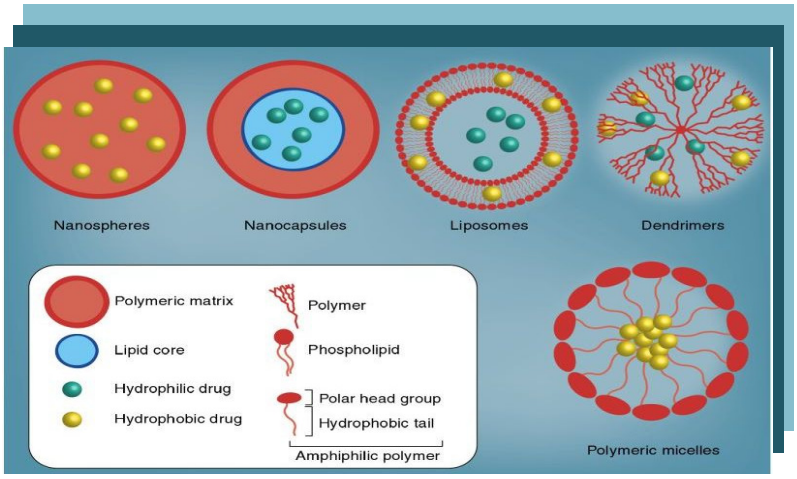

Figure 10 - Types of nanocarrier systems for gene delivery [67].

Among the delivery systems depicted in Figure 10 nanocapsules and nanoparticles are one of the most important ones, because they are usually comprised by cationic polymers. Cationic polymers can efficiently condense the nucleic acids into nanometer range complexes, through their positively charged amine groups by electrostatic interaction with the negatively charged phosphate groups of the nucleic acids, thereby masking their negative charge, by

complexation [64, 68]. Nucleic acids are polyanionic molecules with a large hydrodynamic diameter which presents a significant barrier towards efficient cellular uptake [68]. Cationic polymers, apart from condensing RNA molecules to several fold smaller sized structures, also provide a surface positive charge to the complex. In fact, due to their size, nanoparticles can achieve higher intracellular uptake, which may be favorable for improving transfection efficacy when compared to other systems [55]. Also, most cationic polymers bear amine groups that are protonable at acidic pH. This efficient contact between the positively charged polycation molecule and the negatively charged RNA backbone is responsible for the spontaneous formation of polycation-RNA nanoparticles, also known as polyplexes (Figure 11) and it is dependent on the ratio of nitrogen atoms of the polymer to the phosphate groups present in the polynucleotide (N/P ratio) [69].

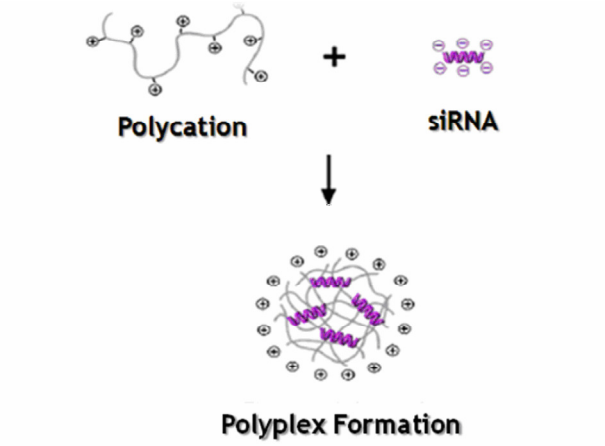

Figure 11 – Formation of polyplexes (Adapted from [70]).

Given their polymeric nature, cationic polymers can be synthesized in different lengths, with different geometry (linear versus branched), and with substitutions or additions of functional groups with relative ease and flexibility. This opens the way to extensive structure/function relationship studies [71]. The physicochemical properties of positive surface charge (at N/P > 1) and nanoscale particle form facilitates electrostatic cellular membrane interaction and uptake, nuclease degradation protection and permits size-mediated extravasation across vasculature endothelial barriers into tissue [72]. Despite the diversity of materials at the disposal for synthesis of nanoparticulated systems PEI and chitosan-based nanocarriers have been gaining an exponential interest as non-viral gene delivery systems, mainly due to its unique properties [70].

Polyethylenimine (PEI), a polycationic polymer has emerged as one of the most promising candidates for the development of efficient gene delivery vectors, namely for RNA delivery, due to its cationic charge density potential [73]. Polyethylenimine exists as both a branched

and linear structure. Synthesis of branched polyethylenimine (B-PEI) proceeds via acid-catalyzed polymerization of aziridine whereas the linear structure (L-PEI) is synthesized via ring opening polymerization of 2-ethyl-2-oxazoline followed by hydrolysis (Figure 12) [74].

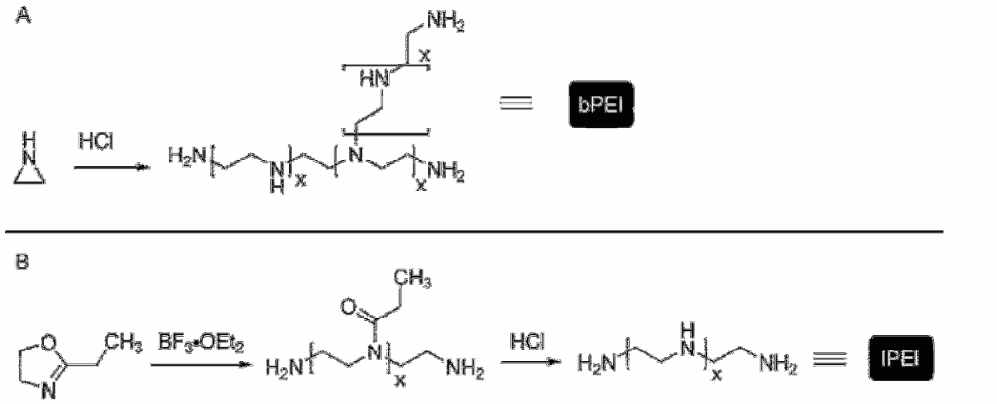

Figure 12 - Synthesis of PEI by (A) Acid-Polymerization of Aziridine to Yield B-PEI and (B) Ring-Opening Polymerization of 2-Ethyl-2-oxazoline followed by Hydrolysis to Yield L-PEI) (Adapted from [74]).

The complexes PEI-nucleotide show high stability, controllable size, adjustable unpackaging properties in cells, and flexibility for addition of moieties that target specific entities on cell membranes and intracellular structures. Many factors affect the efficiency/cytotoxicity profile of PEI polyplexes (and almost all non-viral vector) such as molecular weight, degree of branching, ionic strength of the solution, zeta potential and particle size [75]. Branched PEI (B-PEI) and linear PEI (L-PEI) can both be used effectively for gene delivery. Although L-PEI is generally preferred for *in vivo* applications because of its low toxicity profile, B-PEI contains a higher percentage of primary amines and is thus more suitable for modifications. B-PEI contains primary, secondary and tertiary amines in a ratio of 1:2:1 with pKa values around the physiological pH. The primary amines are mainly responsible for high degree of RNA binding, but they also contribute to toxicity during transfection, while the secondary and tertiary amino groups provide good buffering capacity to the system [74]. In general, PEI has potential as a siRNA carrier due to its superior transfection efficiency which can facilitate endosomal escape after entering the cells as it acts as a "proton sponge" during acidification of the endosome. In addition, PEI presents a high pH buffering capacity over the range of pH that is believed to enhance the exit from the endosomal compartment [5]. However, the high toxicity of PEI is one of the major limiting factors especially for *in vivo* use. Polymers with low molecular weight (< 25KDa) display low toxicity, but the transfection efficiency is low as

well. It is commonly believed that the most suitable molecular weight of PEI for gene transfer ranges between 5KDa and 25KDa.

Additionally, chitosan (CS) is one of the most widely used cationic polymers for nucleic acids delivery. Chitosan has wide applications in pharmaceutical industry and is produced commercially by the alkaline deacetylation of chitin, which is the structural element in the exoskeleton of crustaceans (shrimp, crabs, etc) and cell walls of fungi. CS is a copolymer of repeating D-glucosamine (deacetylated unit) and N-acetyl-D-glucosamine (acetylated unit) monomers, linked via β(1-4) glycosidic bonds (Figure 13) [64].

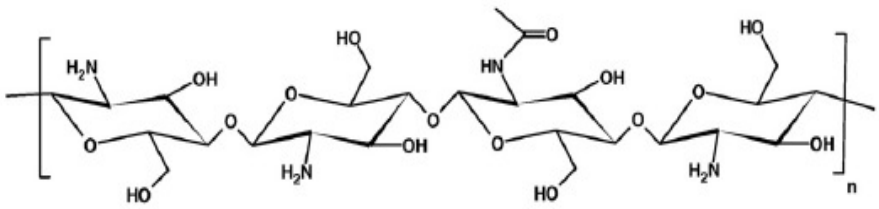

Figure 13 - Chitosan chemical structure (Adapted from [76]).

CS is a weak base with a pKa value of the deacetilated unit of approximately 6.5, however it is insoluble at neutral and alkaline pH values but soluble in an acidic medium, which greatly limits its further biomedical applications [76, 77]. At physiological pH, the amino groups on chitosan are only partially protonized limiting the interactions between chitosan and siRNA [64]. Therefore, the main characteristic of chitosan that accounts for its potential as a gene delivery vehicle is its cationic nature [78]. Curiously, the most important characteristic of CS is due to the primary amine groups present in its backbone, since below the pKa they become positively charged [76]. CS is also considered to be a good candidate for gene delivery, since it has beneficial qualities such as low toxicity, low immunogenicity, non inflammatory, excellent biodegradability, biocompatibility, as well as a high positive charge than can easily form polyelectrolyte complexes with negatively charged nucleotides by electrostatic interaction [5, 77, 79]. The protonated amine groups allow transport across cellular membranes and subsequent endocytosis into cells [80].

Recently, poly(allylamine) (PAA), a synthetic cationic polymer having high density of primary amino groups, has drawn considerable attention as a non-viral gene delivery system (Figure 14) [81]. PAA carries a strong positive charge, which enables it to bind and package negatively charged RNA. It is a pH-sensitive polymer, extensively used in the fabrication of biocompatible films, nanomaterials and for cell encapsulation. However, the cytotoxicity of

PAA, owing to its strong polycationic character, has severely restricted its use as a gene delivery system [82].

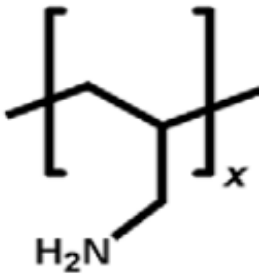

Figure 14 – Poly(allylamine) chemical structure (Adapted from [83]).

To reduce its cytotoxicity, Boussif *et al*. (1999) modified PAA with hydrophilic methyl glycolates and found that its ability to mediate gene transfer into cells increased by several orders of magnitude concurrent with decreased cytotoxicity [84]. More recently, Pathak *et al*. (2007) substituted primary amino groups of PAA (17 kDa) with imidazolyl moieties, which are presumed to enhance endosomal release, and improve its gene delivery efficiency [81].

The aim of the study is to compare the performance of these different condensing polycations on sRNA condensation, in a model system, with the subsequent assess of biophysical and structural characteristics (such as size, zeta potential, morphology and complex stability) of the polymer-sRNA complexes, in order to achieve a successful delivery system for sRNA.

CHAPTER II

Materials and Methods

2.1 Materials

Nutrient Broth medium used to grow the bacterium *R. sulfidophilum* DSM 1374 (BCCM/LMG, Belgian) was obtained from LIOFILCHEM (Italy). NaCl and isopropanol from Panreac (Barcelona, Spain) was used. Guanidinium salt and all the chemicals used in the lysis buffer were obtained from Sigma-Aldrich (St Louis, MO, USA). All solution were freshly prepared using 0.05 % Diethyl pyrocarbonate (DEPC) treated water. DEPC was purchased in Fluka (Sigma). Five different polycations were used. CS low molecular weight (LMW) (M_w = 50–190 KDa; degree of deacetylation ranged from 75-85 %), CS medium molecular weight (MMW) (M_W = 190–310 KDa; degree of deacetylation ranged from 75-85 %), Linear-PEI (M_w = 1300 Da, 50 wt % in H_2O) and PAA (M_w = 17 KDa; 20 wt % in H_2O) were obtained from from Sigma-Aldrich (St Loius, MO, USA). Branched-PEI of M_w = 10 KDa was purchased from Polysciences, Inc. (Warrington, PA). They were used in the experiments according to the instructions. Fetal bovine serum (FBS) was purchased from Biochrom and Heparin (25000 IU for 5 mL) was obtained from Winthrop. The DNA molecular weight marker was obtained from Vivantis Technologies (Oceanside, CA, USA). The compounds used in protein analyses were BSA from Sigma (St Louis, MO, USA) and low molecular weight protein markers from GE Healthcare, Sweden. All salts used in this research were of analytical grade. All the solutions used in the experiments were made up in RNase-free conditions.

2.2 Methods

2.2.1. Bacterial *R. sulfidophilum* DSM 1374 growth conditions

The marine photosynthetic bacterium *R. sulfidophilum* DSM 1374 strain was used in this study. For pre-cultivation, a stride from a selective plate was inoculated into a shake flask containing Nutrient Broth (g per liter of deionized water: beef extract, 1; yeast extract, 2; peptone, 5 and sodium chloride, 5) supplement with 1% NaCl and pH 6.8. Pre-culture was harvested in the exponential growth phase, i.e., after approximately 8-10 h of cultivation at

30 ºC, at 250 rpm. The overnight pre-culture was used to inoculate fresh NB medium and growth was carried out in 500 mL shake flasks containing 100 mL of Nutrient Broth, in a rotary shaker at 250 rpm under aerobic conditions for 3 days in the dark. Cell growth was evaluated by measuring the optical density of the culture medium at a wavelength of 600 nm (OD_{600}), after dispersing cell flocs by vortexing for 30 s. In all studies performed, the cultures were started with an OD_{600} of approximately 0.01. In order to analyze the influence of culture conditions, different pH, temperatures and NaCl concentrations were evaluated. For each different culture condition tested, three independent fermentation runs were performed. At 2 h intervals, 1 mL of the culture was recovered asseptically for further analysis.

2.2.1.1. Effect of temperature in bacterium growth

R. sulfidophilum was grown at two temperatures 30 and 37 ºC until the early stationary phase was reached, using the medium and culture conditions described above.

2.2.1.2. NaCl concentration effect

To evaluate the effect of NaCl concentration on growth, *R. sulfidophilum* DSM 1374 was inoculated and incubated at 30 and 37 ºC in Nutrient Broth medium with pH adjusted to 6.8 containing NaCl concentrations of 1, 2, 3 and 5 % (w/v).

2.2.1.3. pH effect

These experiments were performed with pH of 6.0; 6.8; 7.5 and 8.5. The pH was adjusted with 0.1 to 1 M HCl and NaOH before autoclaving. Growth was performed at 30 ºC with the medium described above, supplemented with 3 % NaCl.

2.2.2. Precipitation of extracellular nucleic acids

The isolation of extracellular nucleic acids was based on the method described by Martins et al. (2010) with some modifications [85]. 1 mL of *R. sulfidophilum* DSM 1374 culture medium was recovered by centrifugation at 10.000 g for 10 min at 4 ºC. The bacterial *pellets* were discarded and the supernatants were transferred very carefully to a clean tube. The nucleic acid fraction in the supernatant was precipitated by adding 1 mL of ice-cold isopropanol. After incubating on ice for 10 min, the nucleic acids were recovered by centrifugation at

10.000 g for 10 min at 4 ºC. The nucleic acids *pellets* were air-dried for 5 min at room temperature and their solubilization was performed in 200 µL of 0.05% DEPC-treated water. Finally, 260 and 280 nm absorbance of the samples was determined using Nanodrop spectrophotometer to assess RNAs quantity and purity.

2.2.3. Agarose gel electrophoresis

The nucleic acids fractions and the samples of polycation/sRNA nanoparticles in different ratios (20 µL) were analysed by horizontal electrophoresis using 1.5 % and 0.8 % agarose gels, respectively (Hoefer, San Francisco, CA, USA). The electrophoresis was carried out in Tris-acetic acid (TAE) buffer in DEPC-treated water (40 mM Tris base, 20 mM acetic acid and 1 mM EDTA, pH 8.0) and runed at 90 V for 50 min for nanoparticles and at 100 V for 35 min for nucleic acids. The bands corresponding to nucleic acids and sRNA–nanoparticles complexes were visualized under ultra violet light after staining the gels with ethidium bromide (0.5 µg/mL) or a total of 5 µL of a 10000x solution of Gelstar. The gels were visualized under UV light in a Vilber Lourmat system (ILC Lda, Lisbon, Portugal).

2.2.4. Protein analysis

2.2.4.1. Protein concentration

Protein content of each sample was measured by using a modification [86] of the micro-BCA (bicinchoninic acid) assay (Thermofisher scientific Inc.) described by Pierce. A fraction of each sample (10 µL) was added to 200 µL of BCA reagent in a microplate and incubated for 30 min at 60 ºC. After cooling the microplate to room temperature, absorbance was measured at 570 nm in a microplate reader. The calibration curve was prepared using Bovine Serum Albumin standards (10 µg/mL–100 µg/mL) (Figure 1).

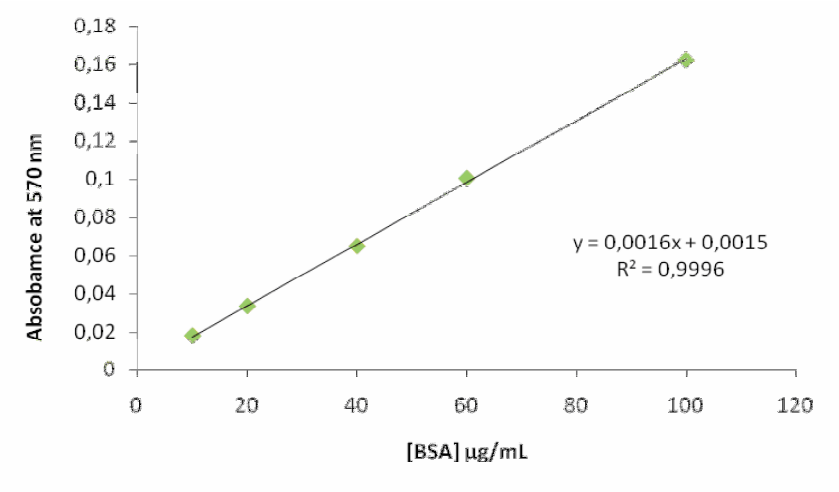

Figure 1 - Reference curve Bovine Serum Albumin standards (10 µg/mL-100 µg/mL).

2.2.4.2. SDS-PAGE

In order to observe the general characterization of the existing proteins, the fractions containing proteins were identified by sodium dodecyl sulfate-polyacrylamide gel electrophoresis (SDS-PAGE) analysis. SDS-PAGE was performed according to the method of Laemmli [87] with 15 % of polyacrylamide gel. Samples were desnatured by the addition of loading dye containing 500 mM Tris-HCl (pH 6.8), 10 % SDS, 0.02% bromophenol blue (w/v), 0.2% glycerol (v/v), 0.02% ß-mercaptoethanol (v/v), followed by incubation at 100 ºC for 5 min. The electrophoresis was carried out in 4 % stacking and 12.5 % resolving gels, with an electrode buffer containing 25 mM Tris-HCl, 192 mM glycine and 10 % SDS and was run at 150 V for 90 min.

2.2.5. Bacterial *E. coli* DH5α and growth conditions

The model sRNA used for the study of polyplexes was obtained from a cell culture of *E. coli* DH5α. Growth was carried out in 1 L shake flasks containing 250 mL of Terrific Broth (tryptone, 12 g/L; yeast extract, 24 g/L; glycerol, 4 mL/L; KH_2PO_4, 0.017 M and K_2HPO_4, 0.072 M), in a rotary shaker at 250 rpm at 37 ºC. It was suspended in the late log phase ($OD_{600} \approx 9$). Cells were recovered by centrifugation and were stored at -20 ºC.

2.2.6. Lysis and sRNA isolation of *E. coli* DH5α

Cells were lysed and sRNA was extracted using the acid guanidinium thiocyanate-phenol-chloroform method described by Chomczynski and Sacchi [88] with some modifications. To perform the lysis, 50 mL of bacterial *pellet* were resuspended by successive pipeting in 5 mL of Solution D (4 M guanidinium thiocyanate; 25 mM sodium citrate, pH 4.0; 0.5 % (m/v) N-laurosylsarcosine (Sarcosyl); and 0.1 M ß-mercaptoethanol). After incubating on ice for 10 min, cellular debris, genomic DNA and proteins were precipitated by gently adding and mixing 1 mL of 2 M sodium acetate (pH 4.0) and 5 mL of water-saturated phenol. The sRNA isolation was achieved by adding 1 mL of chloroform/isoamyl alcohol (49:1), and by mixing vigorously until two immiscible phases were obtained. After incubating for 15 min on ice, sRNA was recovered by centrifugation at 10.000 g for 20 min at 4 ºC. The upper aqueous phase, which contained mostly RNA, was recovered and concentrated by the addition of 5 mL of ice-cold isopropanol. The precipitate was recovered by centrifugation at 10.000 g for 20 min at 4 ºC. The sRNA *pellet* was resuspended in 1.5 mL of Solution D. It was concentrated again with 1.5 mL of ice-cold isopropanol. After centrifuging for 10 min at 10.000 g (4 ºC), the sRNA *pellet* was washed with 2.5 mL of 75 % ethanol and incubated at room temperature for 10 min, followed by a 5 min centrifugation at 10.000 g (4 ºC). The air-dried *pellets* were dissolved in 500 µL of 0.05 % DEPC-treated water and incubated 10 min at room temperature to ensure complete solubilization. Finally, the optical density of the samples was determined using Nanodrop spectrophotometer to assess RNAs quantity and purity.

2.2.7. Particles formation

All the polyplexes were formulated using the method of simple complexation between molar concentrations of positive charge, present in the protonated amine groups of polycation (N), and negative charged of the phosphate groups of RNA (P), as it was previously reported in the literature [70, 89]. To determine specific N/P ratio, the mass of 325 Da corresponding to one phosphate group on sRNA was used. Moreover, over the pH used in this study, RNA does not suffer ionization because it contains an almost constant anionic charge density, with the pKa of the respective phosphate group of 1.5 [90]. The calculation of positive charges of the monomers was made in accordance with the pKa values and molecular weight described for each polymer (Table 2, Chapter III). sRNA stock solution was prepared by sRNA dissolution in sodium acetate buffer (0.1 M sodium acetate/0.1 M acetic acid, pH 4.5), up to a final concentration of 25 µg/mL. The sRNA concentration was determined by UV absorbance at 260 nm. A solution of 40 ug/ml of RNA will have an absorbance of 1. The polycations stock solutions were also prepared in sodium acetate buffer pH 4.5 in a concentration of 10 mg/mL.

Preliminary experiments were performed to identify the concentration range where the nanoparticles were formed. A fixed volume of Polycation solution (100 µL) of variable concentration was added to a solution containing RNA (400 µL). The final concentration of RNA was equal to 20 µg/mL (60.6 µM) and was kept constant in all the methods used for the characterization of the RNA-Polycation complexes. Particles were obtained by addition of cationic polymer solution to siRNA solution and immediately vortexed at maximum speed for 30 s. All the samples were subsequently left for equilibration at room temperature for 60 min.

2.2.8. Circular Dichroism

Circular dichroism (CD) is used to measure the optical activity of asymmetric molecules in solution. CD it is a form of spectroscopy used to determine the optical isomerism and secondary structure of molecules. This technique gives the information about the unequal absorption of left – L and right – handed R circularly-polarized light by optically- active molecule. CD consists on the difference between the absorption of these two components. The quantity used to describe this phenomenon is called ellipticity, Θ, and is expressed in degrees. The molar ellipticity, [Θ] is calculated from the measured Θ using the expression (1)

$$[\Theta] = \frac{\Theta \times 100 \times M}{c \times l} \qquad (1)$$

where Θ is the measured ellipticity in degrees, *c* is the RNA concentration in mg/mL, and l is pathlength in cm, and M is the DNA molecular weight. The application of this technique to study RNA conformations has stemmed from the sensitivity and ease of measures, the non-destructive nature, the fact that conformations can be studied in solution, and the requirement of small amounts of material. CD was used to monitor the RNA behavior when subjected to the different pH values. CD spectra were obtained using a 0.2 cm path length quartz rectangular cell at the constant temperature of 25 °C, a Jasco 1850 spectrofotometer. Spectra were recovered from 215 to 320 nm at a scan speed of 10 nm/min and a bandwidth of 1 mm. Three spectra were accumulated and averaged for each sample. The final sRNA concentrations were of 100 µg/mL. All measurements were conducted under a constant gas flow, to purge the ozone generated by the light source of the instrument. The CD signal was converted to molar ellipticity, smoothed with a Jasco Fast Fourier transform algorithm.

2.2.9. Determination of Deacetylation Degree

The first derivative ultraviolet spectrophotometry (1DUVS) is a technique used for determination of the DD of chitosan samples in acidic solutions. This technique is based on the measurement of the height (H) of the maximum absorbance value of N-acetyl-D-glucosamine residues in the polymer backbone to address the percentage of the primary amine groups. The determination of the DD degree and the acetic acid solution spectra was performed as previously described [85] with some modifications. Briefly, the spectra of acetic acid solutions with different concentrations from 0.01 M to 0.03 M were obtained using a Shimadzu 1700 Uv-vis spectrophotometer (Shimadzu Corporation, Kyoto, Japan) in the range of 190-240 nm. The first derivative spectra demonstrated the existence of a common point at 203nm, denoted as the zero crossing point (ZCP). Afterwards a sequence of N-acetyl-D-glucosamine standard solutions of 0.005 – 0.050 mg/mL in a 0.01 M acetic acid were prepared and their first derivative spectra registered as denoted in Figure 2A. The superimposition of the ZCP spectra and the N-acetyl-D-glucosamine allowed the measurement of the maximum H value at 203 nm. A linear calibration curve was consequently obtained by plotting the H_{203} values versus the corresponding N-acetyl concentration as depicted in Figure 2B.

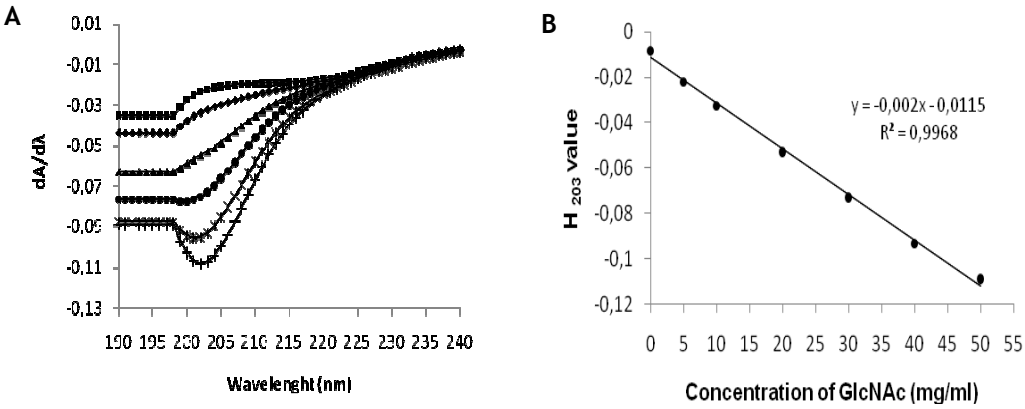

Figure 2 - 1DUVS *N*-acetyl-D-glucosamine spectra and reference curve. A) First derivative spectra of the of *N*-acetyl-D-glucosamine solutions (■ - 0.005 mg/mL; ♦ - 0.01 mg/mL; ▲ - 0.02mg/mL; ● - 0.03mg/mL; * - 0.04mg/mL; + - 0.05mg/mL); B) Reference curve *N*-acetyl-D-glucosamine.

To determine the DD, 0.01 g of chitosan samples were dissolved in 10 mL of 0.01 M acetic acid and diluted in 90 mL of ultrapure water as described by Tan and colaborators, 1998 [91]. The first derivative spectra of the chitosan materials were recorded and the H_{203} value was measured. The DD of the different samples was determined as follows:

$$DD\ (\%) = \left[1 - \left(\frac{A}{\frac{(10 \times W) - 204\,A}{161} + A}\right)\right] \times 100 \qquad (2)$$

204 – Molecular weight of *N*-acetyl-D-glucosamine

161 – Molecular weight of D-glucosamine

A – Amount of *N*-acetyl-D-glucosamine

W – Mass of the chitosan sample

2.2.10. Determination of the encapsulation capacity of sRNA

The sRNA encapsulation efficiency (EE) is an important parameter to be determined during the encapsulation of biomolecules in the nanoparticulated systems. It is important to clarify this factor, in order to establish a relation of the sRNA weight loaded into the nanoparticles as demoted the equation. The EE of the sRNA entrapped or adsorbed onto the nanoparticles was calculated from the determination of free sRNA concentration in the supernatant recovered after particle centrifugation (15.000 g, 20 min, 25 °C). The amount of unbounded sRNA was determined by UV-Vis analysis (Shimadzu UV-Vis 1700 spectrophotometer) at 260 nm. Supernatant recovered from unloaded polycation (without siRNA) was used as a blank. Three repetitions of this procedure were performed for each system. The encapsulation efficiency was calculated as follows:

$$EE\ (\%) = \frac{Amount\ Total\ sRNA - Amount\ of\ unbound\ sRNA}{Amount\ of\ Total\ RNA} \times 100 \qquad (3)$$

2.2.11. Observation of polyplexes morphology using SEM

The morphological characteristics of the nanoparticles were visualized with scanning electron microscopy (SEM) (Hitachi S-2700, Tokyo, Japan). Briefly, the particle samples were resuspended in 100 µL of ultrapure water and stored at 37 ºC overnight. Afterward, one drop of the nanoparticle samples was added to 16 mm cover glasses and mounted on aluminum boards using a double-sided adhesive tape. The samples were then sputter coated with gold using an Emitech K550 Sputtering Coater (London, England) for 3 min at 30 mA before viewing under SEM.

2.2.12. Determination of surface charge of polyplexes

The surface charges (zeta potential) of the particles were determined by laser Doppler electrophoresis using a Zetasizer Nano ZS (Malvern Instruments Ltd., U.K.). Samples were prepared as previously described. Measurements were carried out in a folded capillary electrophoresis cell (Malvern Instruments) at room temperature. The average values of zeta potential of nanoparticles were calculated with the data obtained from three measurements ± SD, in automatic mode.

2.2.13. Measurement of the hydrodynamic diameter of the polyplexes

The mean particle size (mean particle diameter, z average) of polyplexes and polydispersion index were determined by dynamic light scattering (photon correlation spectroscopy, PCS) using an N5 Particle Analyzer (Beckman Coulter Inc., U.S.A.). Particle diameters of the freshly prepared complexes were measured at 25 °C, and data were collected at 90 ° scattering angle. The time-averaged autocorrelation functions were transformed into intensity-weighted distributions of the apparent hydrodynamic diameter using the available Malvern PCS software 6.20. Mean hydrodynamic diameters were calculated for size distribution by weight, assuming a lognormal distribution, and the results were expressed as mean ± SD of three runs. The sizing data had a polydispersity index less than 0.5.

2.2.14. Protection and release of encapsulated sRNA

The protection and release profile of the encapsulated sRNA was during the delivery process by 0.8 % agarose gel electrophoresis, to examine the structural integrity of sRNA. All the

polyplexes were resuspended in PBS buffer, pH 7.4. The protection experiments were carried out by incubation of 12.5 µL of polyplexes with 1.5 µL of RNase solution (10 and 100 µg/mL) for 1 h at 37 ºC or with 10 % fetal bovine serum (FBS) for 30 and 60 min at 37 ºC. To characterize the release of the encapsulated sRNA, the nanoparticle samples were incubated with a series of heparin solutions (0.01, 0.1, 0.5 and 1 IU/mL of heparin ammonium salt) prepared by diluting aliquots of a heparin stock solution (10 IU/mL). The polyplex solutions (10 µL) were incubated with 10 µL of each heparin concentration for 1 h at 37 ºC.

CHAPTER III

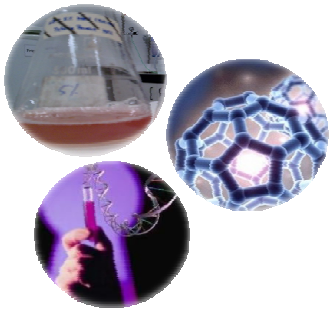

Results and Discussion

For the improvement of the biological effect in RNAi-based therapies, it is required the development of new vehicles capable of transposing the biological barriers and to protect RNA. Different methodologies have been developed for infusing exogenous RNAi molecules into the cytoplasm of cells, being the chemical-based methods the most widely used [8]. The development of polymeric nanodevices that combine the preeminent features of traditional delivery vectors, but offer new flexibility to overcome some of the biological boundaries is gaining momentum [35]. Actually, it has been demonstrated that these types of nanodevices provide safe and efficient delivery of siRNAs [92]. Thus, suitable vehicles will also be developed to achieve higher transfection efficiencies and siRNA protection.

In this way, the main goal of this thesis is to assemble a new strategy to biosynthesize sRNA using the bacterium *Rhodovulum sulfidophilum* DSM 1374, resulting in the improvement sRNA production and quality, in order to obtain a less time-consuming and economics procedure. In addition, suitable vehicles will be developed to efficiently deliver the siRNA to the cells, particularly into the cytoplasmic compartment, the location where their function is exerted, which usually is a critical barrier to an efficient therapeutic response. The *R. sulfidophilum* DSM 1374 was used due to its ability to secrete RNA to the extracellular medium and because there is no evidence of bacterium RNases in the culture medium, as well. Therefore, these are great advantages for the recovery and application of sRNA molecules. Moreover, DSM 1374 strain presents an advantage in relation to the strain PS88 because it is not necessary to perform lengthy and expensive processes for its isolation from environment sources. Since the DSM 1374 strain is commercially available, it allows a wider and simplest use in bacteria characterization or in application studies. However, this strain is not totally characterized concerning its optimal growth conditions for sRNAs production over cultivation time, when compared with the DSM 2351 strain.

Section I

Effects of temperature, pH and NaCl concentrations on R. sulfidophilum growth

In this study some basic bacterium growth parameters such as temperature, pH and NaCl concentrations were evaluated in aerobic conditions. Moreover, we intend to attain the best bacterium growth conditions combined with a maximum efficiency of extracellular sRNA production. In most of the studies, this bacterium was grown in anaerobic conditions and in presence of light, at 25 or 30 ºC, in RCV or PYS medium supplemented with NaCl and in some cases at 100 rpm shaking [56, 93-95]. Briefly, in this study *R. sulfidophilum* DSM 1374 strain was cultivated in shake flasks at 250 rpm using Nutrient Broth medium under aerobic conditions, in the dark, for 3 days. The growth experiments have shown that cultivation under aerobic conditions was more effective, allowing higher growth rates and optical densities than in anaerobic conditions. These results are in accordance with literature, since the bacterium *R. sulfidophilum* DSM 1374 is facultative phototrophic, so it is able to grow anaerobically in light or aerobically in the dark [56, 96]. In addition, the growth in aerobic conditions does not require specific laboratory material and it is easier to handle.

In fact, some initial experiments showed that the cultivation in Nutrient Broth (NB) medium was more effective, conducting to higher optical densities than with other media, such as Brain Heart Infusion (brain heart infusion, 17.5 g/L; peptone, 10 g/L; glucose, 2 g/L; disodium phosphate, 2.5 g/L and sodium chloride, 5 g/L), Mueller Hinton (meat extract, 2 g/L; casamino acids, 17.5 g/L; starch, 1.5 g/L; calcium chloride, 0.1 g/L and magnesium chloride, 0.2 g/L) and Tryptone Soya (tryptone, 15 g/L; papaic digest of soybean meal, 5 g/L and sodium chloride, 5 g/L), which are the manufacturer´s recommended media for *R. sulfidophilum* DSM 1374 growth (Figure 1). This result could be associated to the fact of the NB be the richest medium, due to the conjugation of components such as yeast and beef extract, that serve as carbon and nitrogen source.

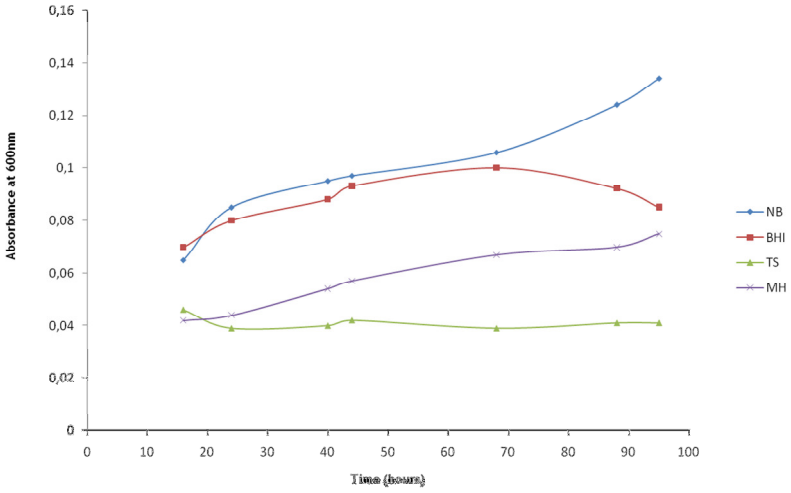

Figure 1 - Effect of several mediums on growth of the photosynthetic bacterium *R. sulfidophilum* DSM 1374 that it was cultivated under aerobic conditions in the dark at 30 °C.

Based on this initial finding, all the experiments performed to evaluate the influence of other environmental parameters were developed using the NB culture medium. The temperature and NaCl supplementation experiments were carried out by incubating the *R. sulfidophilum* DSM 1374 at two different temperatures, 30 and 37 ºC, using the NB medium supplemented with NaCl concentrations ranging from 1 to 5 % (w/v) (1, 2, 3 and 5 %). The effect of NaCl concentration and temperature in *R. sulfidophilum* is shown in Fig. 2 and 3. In general, the growth was slightly lower at 37 ºC (Figure 3) than at 30 ºC (Figure 2), which is consistent with the optimum growth temperature of *R. sulfidophilum* (30 to 35 ºC) reported by other authors [43, 44]. In detail, Figure 2 shows that the bacterium was not able to grow with 1 % NaCl. However, when using NaCl concentrations of 2, 3 and 5 % higher growth rates were achieved. At 1 % NaCl the growth curve is constant with no exponential phase. Similar results were also obtained for 1 and 2 % NaCl at 37 ºC (Figure 3). As occurs with an essential medium component, the NaCl concentration was found to significantly affect the bacterium growth.

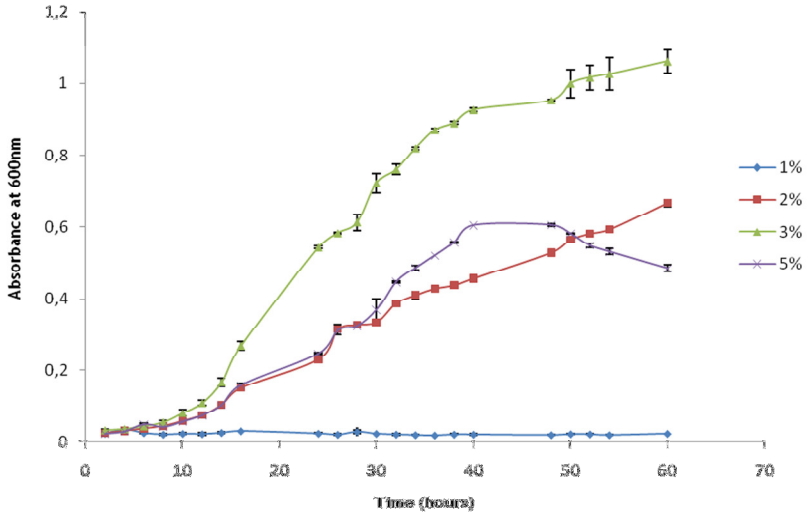

Figure 2 - Effect of NaCl concentration on growth of the photosynthetic bacterium *R. sulfidophilum* DSM 1374 that it was cultivated in nutrient broth medium supplemented with different NaCl concentrations (1, 2, 3 and 5 %) under aerobic conditions in the dark at 30 ºC. The data presents the average of 3 times duplicate cultivations. Bars in figure indicate standard deviation.

At 30 ºC (Figure 2), *R. sulfidophilum* DSM 1374 was able to grow in NaCl concentrations of 2 to 5 %, being verified an optimum growth at 3 %. This salt concentration promotes the bacterium growth to reach optical densities of 1.061 after 60 h of cultivation. Nevertheless, using the NaCl concentration of 5 % the stationary phase occurred earlier, after 48 h of cultivation and a maximal optical density obtained was of 0.605. In the experiment using 2 % NaCl, it was verified that the bacterium also grew well however, the highest optical density attained was 0.676. Together, these results demonstrate that using the temperature of 30 ºC the best NaCl concentration for *R. sulfidophilum* DSM 1374 growth is 3 % and an increase to 5 % decreases the growth. This fact suggests that this strain has halotolerance up to 3 % NaCl. Similarly, some studies with *R. sulfidophilum* described an optimal NaCl concentration of 2.5 % [97] for favorable growth however, the authors pointed out that higher salt concentrations also allow the bacterium to growth. In fact, the results obtained in our study are in accordance with Hansen and Veldkamp [44], since the best growth occurred with 3 % NaCl, which is very close to the values described by the authors as optimal NaCl concentration (2.5 % NaCl). Recent works developed to optimize the bacterium PS88 growth have employed the aerobic culture in the dark, at 30 ºC for 10 days and the maximum growth was achieved when using NaCl concentration between 1 and 2 % [46]. Additionally, Ando and colleagues (2009) showed that *R. sulfidophilum* DSM 2351 could grew anaerobically at 30 ºC, resulting in optical densities around 0.6 after 60 h of growth [52]. In comparison, our results suggest that the described

conditions enabled a shorter cultivation time (approximately 24 h) reaching higher cell density.

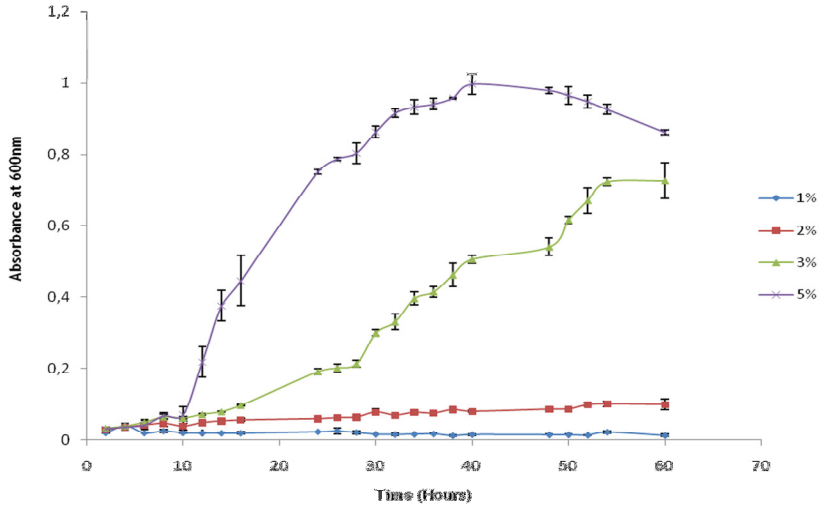

Figure 3 – Effect of NaCl concentration on growth of the photosynthetic bacterium *R. sulfidophilum* DSM 1374 that it was cultivated in nutrient broth medium supplemented with different NaCl concentrations (1, 2, 3 and 5 %) under aerobic conditions in the dark at 37 ºC. The data presents the average of 3 times duplicate cultivations. Bars in figure indicate standard deviation.

Otherwise, at 37 ºC (Figure 3), *R. sulfidophilum* DSM 1374 was able to grow only in the presence of NaCl concentrations of 3 and 5 % with an optimum growth at 5 %. At this NaCl concentration the maximum optical density was 0.998 after 48 h incubation (stationary phase). These results can also be supported by the hypothesis of halotolerance, since this bacterium also grew on non-optimal conditions, namely using 37 ºC and 5 % NaCl, as described by Watanable et al. (1998) for PS88 strain [43, 53, 98]. Nonetheless, this environment could possible led to an osmotic stress causing an earliest cell death. The exposure of the bacterium to conditions of hyperosmolarity may have increased the cytoplasmic volume as a consequence of an osmotic adjustment by the cells. As a result, there is a decrease in the bacterium cytoplasmic water activities and consequently some essential cellular functions becomes impaired [97, 99].

As described above, we have obtained better growth at 30 ºC with 3 % NaCl, so the studies performed to verify the influence of pH in bacterium growth were developed in nutrient broth medium under these growth conditions (Figure 4).

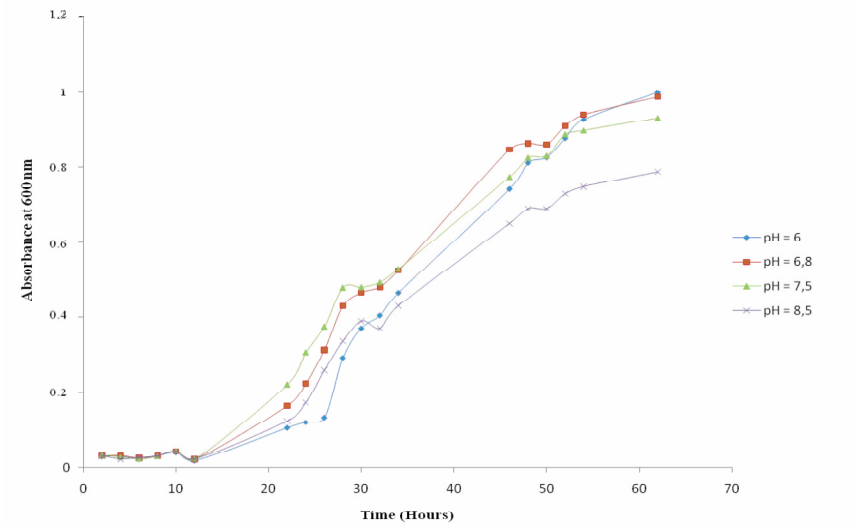

Figure 4 - Effect of pH on growth of the photosynthetic bacterium *R. sulfidophilum* DSM 1374 that was cultivated in nutrient broth medium supplemented with 3 % NaCl under aerobic conditions, in the dark, at 30 ºC.

According to the literature, *R. sulfidophilum* DSM 1374 is described to grow in the pH range between 7.5 to 9.0, with an optimum pH of 8.0 or 8.5 [43]. However, under the optimized growth conditions, the microorganism grew in pH between 6.0 and 8.5, with an optimum pH of 6.8 (OD_{600} = 0.988). The overall effect of pH on the maximal cell density was not significantly pronounced, being verified a slight growth decrease at pH 8.5 (OD_{600} = 0.788). Therefore, the further growth experiments were performed at pH 6.8.

In general, the experiments performed with the aim of understanding the effect of temperature, pH and NaCl concentration in the DSM 1374 strain growth demonstrated that the best growth is achieved for the culture at 30 ºC in NB medium supplement with 3 % NaCl, pH 6.8 (Figure 2).

Quantity and quality of extracellular sRNA

To elucidate the relation between cell growth and the production of extracellular sRNA, the soluble extracellular nucleic acids were isolated from the culture medium and analyzed during the cultivation. Although, production and function of extracellular nucleic acids have been reported in other strains of the *R. sulfidophilum*, the nucleic acids themselves have not been totally characterized. In this study, we have focused the analysis in the extracellular sRNA fraction of the strain *R. sulfidophilum* DSM 1374. This strain showed relatively rapid

growth and the highest production of the extracellular sRNAs, in comparison with the other described strains of *Rhodovulum* species [46, 52, 55].

After growth of DSM 1374 under the best conditions achieved, using aerobic conditions, in the dark, at 30 ºC with 3 % NaCl (Figures 5A) and 37 ºC with 5 % NaCl (Figure 6A), the extracellular nucleic acids of the culture supernatant were analyzed by agarose gel electrophoresis, after precipitation with isopropanol. Figures 5A and 6A show the nucleic acids profile of the clarified precipitates recovered along the cultivation, containing different RNA species and gDNA. The electrophoresis shows relatively small bands, with high molecular weight corresponding to gDNA. The rRNAs (16S and 23S) bands are also present with molecular weights between 750 to 1500 bp. In addition, sRNAs are present in sharp bands of low molecular weight (below 500 bp). In this study, the main purpose was to evaluate the extracellular sRNAs production along the cultivation curve. Therefore, the set time points of bacterium cultivation were evaluated for nucleic acids production using the software Quantity One (Bio-Rad). This analysis enables a more accurate quantification of the nucleic acids bands present in each sample of *R. sulfidophilum* extracellular medium (Fig. 5B and 6B).

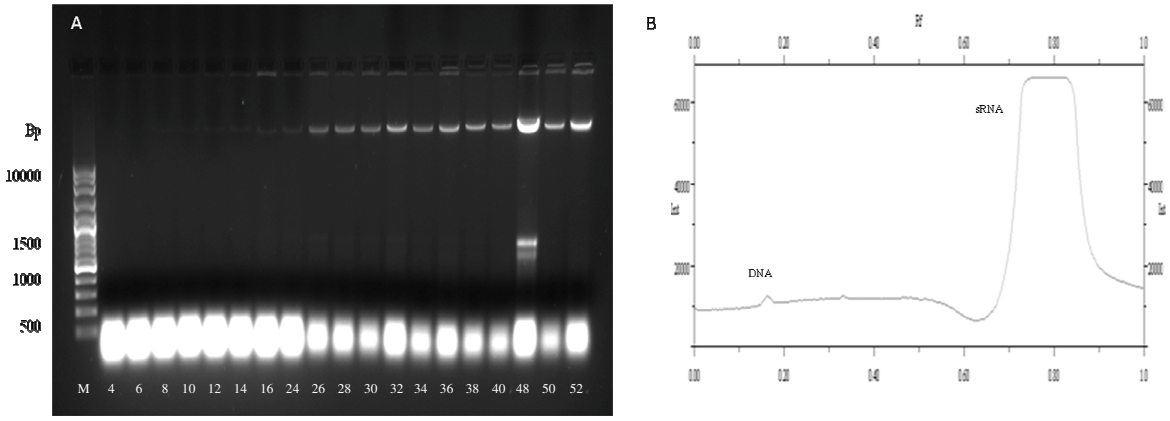

Figure 5 – A) Agarose gel electrophoresis analysis of extracellular medium (after isopropanol precipitation) at 30 ºC with 3 % NaCl. Lane M, molecular weight marker; lane 4 to 16, extracellular sRNAs from 4 to 16 hours of cell growth; lane 24 to 52, extracellular nucleic acids containing gDNA and sRNA molecules from 24 to 52 hours of cell growth. B) Quantity analysis of electrophoresis nucleic acids bands. The graph corresponds to 16 h band showing each nucleic acids bands densities.

The results show different contents of extracellular nucleic acids along the bacterium growth. The production of extracellular sRNAs was demonstrated to increase with the cell growth and they are present in the culture medium since the initial lag phase of 6 or 8 h, as shown in the electrophoresis lanes corresponding to 6 and 8 h (Fig. 5A and 6A). Moreover, in this stage

gDNA is not present and can only be found after 14 h of bacterium growth. These results were confirmed by the intensity of the bands in each sample as it can be representatively visualized by the example graphs resultant from the analysis at 16 h of cultivation (Fig. 5B and 6B), showing intensity peaks corresponding to the nucleic acids produced by the bacterium DSM 1374 at this stage of cultivation.

A significant decrease in sRNAs extracellular production was found after 32 h of growth when the conditions are of 3 % NaCl at 30 ºC and 5 % NaCl at 37 ºC (Figures 5A and 6A, lanes corresponding to 32 h samples). This suggests that the secretion occurs first for low molecular weight molecules, as sRNA, and on the later stages of growth the bacterium initiate the secretion of high molecular weight nucleic acids molecules (gDNA). In figure 5A can also be observed rRNA sub-units (16S and 23S) in later growth phases.

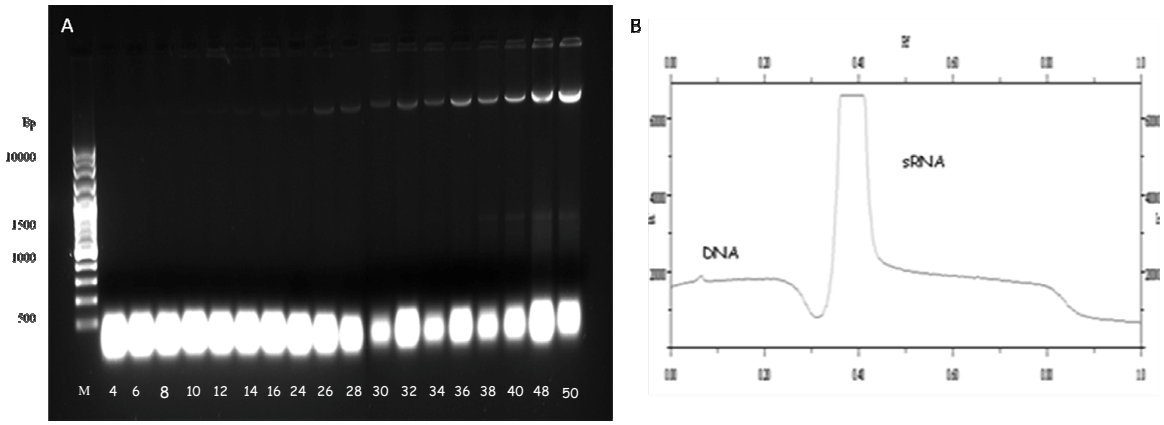

Figure 6 – A) Agarose gel electrophoresis analysis of extracellular medium (after isopropanol precipitation) at 37 ºC with 5% NaCl. Lane M, molecular weight marker; lane 4 to 16, extracellular sRNAs from 4 to 16 hours of cell growth; lane 24 to 50, extracellular nucleic acids containing gDNA, rRNA and sRNA molecules from 24 to 50 hours of cell growth. B) Quantity analysis of electrophoresis nucleic acids bands. The graph corresponds to 16 h band showing each nucleic acids bands densities.

These results confirm once more that the nucleic acids are originated from the active bacterium extracellular production and not from cells autolysis [52]. sRNAs extracellular production is thought to be very beneficial for future development of efficient engineering systems for industrial production of RNA drugs, because harvest and disruption of cells are not necessary.

In summary, we can also conclude that the contaminants species are present in higher quantity at 30 ºC with 3 % NaCl than at 37 ºC with 5 % NaCl, being verified that the secretion of DNA is also noticeably superior in the first growth condition. These data can be a result of

the increased growth in the condition of 3 % NaCl at 30 ºC, since the cell achieve advanced growth stages which can triggers the secretion of other nucleic acids.

In addition, preliminary studies to evaluate sRNA integrity and to confirme sRNA population secreted to the culture medium were performed by denatured polyacrylamide gel electrophoresis analysis (results not shown). The polyacrylamide gel electrophoresis showed the possible presence of tRNAs, however the results were not clear because it is necessary to do further optimizations in the polyacrylamide electrophoresis technique.

Extracellular sRNAs concentrations were estimated by spectrophotometry analysis, measuring absorbance values at 260 and 280 nm. From this quantification also results the 260/280 ratio, which enables the determination of the purity of each sample [100, 101]. The spectrophotometry analysis of extracellular sRNAs recovered after 14 h of *R. sulfidophilum* growth (lag phase) at 30 ºC with 1, 2, 3 and 5 % NaCl presented concentrations of 14 ± 0.2, 62 ± 0.69, 197 ± 0.55 and 97 ± 0.18 µg/mL, respectively (Table 1). For the second temperature tested (37 ºC), the extracellular sRNAs levels produced were lower, being achieved concentrations values of 7 ± 0.46, 22 ± 0.56, 75 ± 0.50 and 175 ± 0.70 µg/mL, at the 14 h of growth.

Table 1 – Quantitative characterization of *R. sulfidophilum* extracellular sRNAs produced in the different growth conditions tested (mean ± SD, n = 3).

	Temperature 30 ºC		*Temperature 37 ºC*	
NaCl (%)	***sRNA (µg/mL)***	***Protein (µg/mL)***	***sRNA (µg/mL)***	***Protein (µg/mL)***
1	14 ± 0.2	9.06 ± 1.81	7 ± 0.46	6.70 ± 1.79
2	62 ± 0.69	8.9 ± 1.56	22 ± 0.56	2.09 ± 2.57
3	197 ± 0.55	22.08 ± 2.16	75 ± 0.50	12.28 ± 2.00
5	97 ± 0.18	6.25 ± 1.06	175 ± 0.70	27.08 ± 2.68

These quantitative results obtained are in accordance with the electrophoresis (Figure 5 and 6) analysis In comparison with the other strains, PS88 has been reported to produce extracellular RNAs in a yield of 62.5 mg/g dry cells or 96.7 mg/L in broth [46, 102] and the DSM 2351 has yield 0.4 µg/mL of extracellular sRNAs in cultivations of 40 h [52]. Therefore, with the conditions described in this study, we are able to obtain a shorter cultivation time

with higher optical density and higher sRNAs production levels, when comparing with the others studies. *R. sulfidophilum* DSM 1374 can produce extracellular natural sRNAs in high yields, reaching 197 ± 0.55 µg/mL, at 30 ºC in NB medium supplemented with 3% NaCl (Table 1). Besides, this strain demonstrates great potential for extracellular RNA production in large quantities, it can also be easily obtained in microbiology manufacturing. Moreover, the time-consuming and labor-intensive handling is not necessary, as this method requires only cultivation of the bacterium for the recovery of sRNA. In addition, the culture volume can be easily scaled up, which is favorable for large-scale industrial preparation.

Recent studies have indicated that many sRNAs play key roles in the regulation of gene expression and they are also expected to be potential candidates for RNA therapeutics [10, 103]. Therefore, the sRNAs must be pure, with no contaminants such as gDNA or proteins, to have biological applicability. For the DNA control, we have already mentioned that its level can be diminished by controlling the culture growth and the recovery of sRNA. Furthermore, the purity of the samples is commonly evaluated by 260/280 nm ratio because it is an indirect method to verify the proteins level. The sRNAs recovered showed a 260/280 nm ratio of 2.0, which is often characteristic of a pure RNA preparation [100]. Nevertheless, a low ratio usually indicates protein contamination due to protein absortion at 280 nm. However, the protein content is a common impurity in RNA preparations that can be omit in spectrophotometry analysis. For this reason, it is necessary a relatively large amount of protein contamination to significantly affect the 260/280 ratio in a RNA solution [104]. For this reason, a more accurate method was used to verify the protein contamination level. Thus the proteins were quantified by the BCA method in sRNA samples with 14 h of cultivation at the different medium conditions, because this contaminant can be overlooked in spectrophotometry analysis. At 30 ºC, protein concentrations of 9.06 ± 1.81, 8.90 ± 1.56, 22.08 ± 2.16 and 6.25 ± 1.06 µg/mL were obtained for the media supplemented with 1, 2, 3 and 5 % NaCl, respectively. At 37 ºC, the proteins produced by the bacterium were achieved to be of 6.70 ± 1.79, 2.09 ± 2.57, 12.28 ± 2.00 and 27.08 ± 2.68 µg/mL, respectively to each NaCl percentage (Table 1). In fact, these results proved that the level of proteins in the sRNA preparation is not high, suggesting that a further purification method could be able to eliminate the remaining proteins.

To identify the proteins profile quantified by micro-BCA method, a SDS-PAGE electrophoresis was also performed (Figure 7). In the electrophoresis it was verified that the proteins are not present in samples of 14 h of cell growth which is in accordance with the ratio of 2.0 ± 0.05 obtained spectrophotometrically (Figure 7, lane 1). In fact, the protein level present in the sRNA fraction, detected by the micro-BCA method, was low during the first 14 h of cultivation, with a maximum value of 27.08 ± 2.68 µg/mL (Table 1). These results are in agreement with results obtained by SDS-PAGE electrophoresis, since in the first lane (lane 1), corresponding to 14 h of cultivation, the protein bands are not visible (Figure 7). On other hand, in the samples obtained from the 40, 48 and 50 h (Figure 7, lanes 5-7) of growth it is

possible to visualize proteins with molecular weights around 40 KDa (Figure 7) and the protein concentration obtained for these samples was also higher.

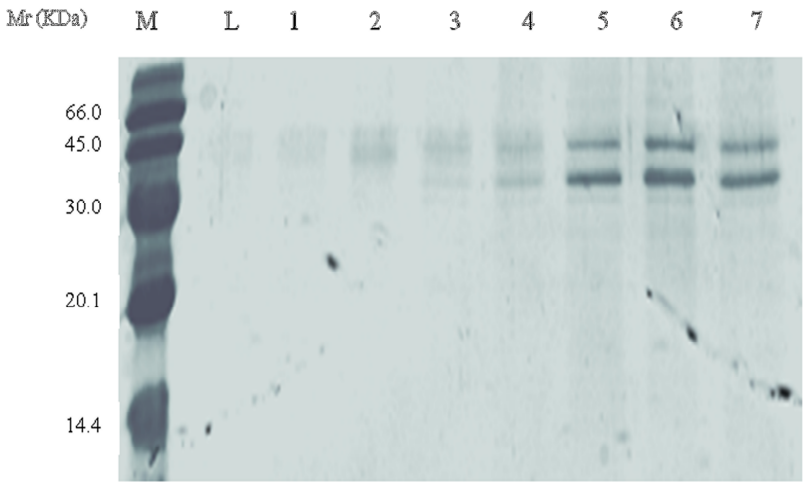

Figure 7 – SDS-PAGE analysis of proteins in nucleic acid samples. Lane M, molecular weight marker; lane L, the medium culture sample; lane 1 and 2, samples at 30 ºC with 1 % NaCl and 14 and 26 h of cultivation, respectively; lane 3 and 4, samples at 30 ºC with 3 % NaCl and 30 and 50 h of cultivation, respectively; lane 5, 6 and 7, samples at 37 ºC with 1 % NaCl and 40, 48 and 50 h of cultivation, respectively.

All the parameters previously referred allowed the assessment of RNA quality, indicating that sRNAs are isolated with high recovery yield and purity. The present study shows that at 14 h of cultivation, a maximum level of 197 ± 0.55 µg/mL sRNA is obtained (Table 1) and a residual protein concentration is achieved. Thus, according to the results obtained in this study, in order to obtain high production of natural sRNA minimizing the impurities, *R. sulfidophilum* DSM 1374 should be cultivate up to 14 h. These experiments with *R. sulfidophilum* DSM 1374 showed relatively rapid growth and the highest production of the extracellular nucleic acids among the strains of Rhodovulum species tested.

Section II

In this section, we will explores the possibility of forming nanoparticles with different polymers using isolated sRNA produced by the bacterium *E. coli* DH5α, and to proceed with the comparison of the physicochemical properties of the polyplexes studied. Carrier systems intended for the transport of the sRNA were prepared using the simple complexation method, forming stable colloids with sub-cellular sizes (< 500 nm). These nanoparticulated systems also demonstrated the ability to condense and entrap sRNA inside a mesh network, when present in different concentrations. This methodology relies on the interaction between negatively charged sRNA and positively charged polycations. The spontaneous formation of the nanoparticles occurs due to intermolecular linkages between the positive and negatively charged species [105], that affect the conformation of both positive and negative species. Increasing the N/P ratio, that is, the number of positive charges associated with the vector particles relative to the intrinsic negative charge of the sRNA, is generally considered to have a beneficial effect for enhancing delivery because the cell entry is facilitated [68]. Moreover, the characteristics of the polyplexes depend on: 1) solution conditions such as ionic strength and solvent polarity; 2) the properties of the nucleic acids, such as length and persistence length; 3) the nature of the polymer (rigidity and charge density), and finally, 4) the preparation protocol (concentration of the respective components, sequence and stirring speed) [106-110]. The several differences observed in the different experiments are addressed in the following section.

Assessment of sRNA conformation at different solutions

First, it was assessed the conformational stability of the sRNA secondary structure in different solutions (H_2O-DEPC and acetate buffer, pH 4.5) using CD (Figure 8). For sRNA in H_2O-DEPC, we observed a positive band around 260 nm and a negative signal at 220 nm. On the other hand, the sRNA spectrum in acetate buffer at pH 4.5 depicts a decrease in the value of the molar ellipticity of the positive band (260 nm) and maintains the negative signal at 220 nm.

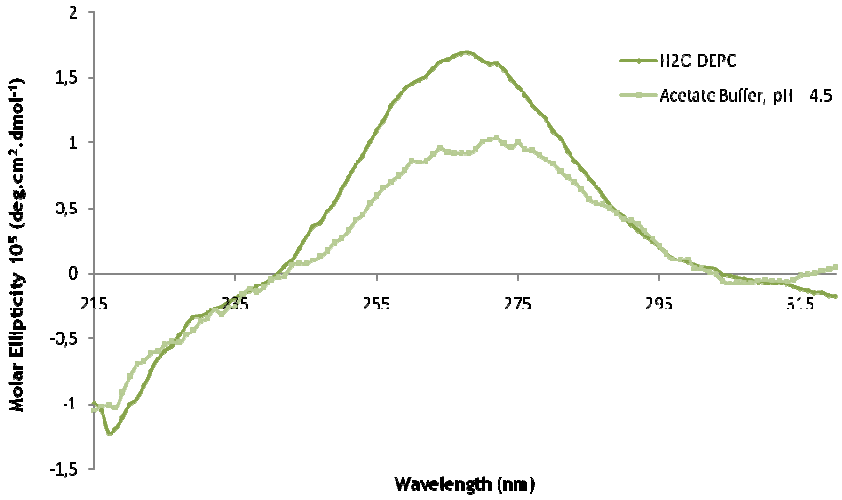

Figure 8 – CD spectra of *E. coli* sRNA in the H_2O-DEPC and acetate buffer, pH 4.5.

These results showed that isolated RNA is sensitive to the buffer used, since the respective CD spectrum is different in acetate buffer and in water. Probably, this indicates that the sRNA structures are influenced at lower pH. However, there is no consensus on the precise nature of the changes that occur in the RNA conformation when the pH is lowered, and consequently pH influences the degree of ionization of sRNA. Biologically, the hybridization occurs naturally in acidic conditions and promotes the neutralization of the condensed phosphate molecules. In *in vitro* this occurs with a pH below 5 and can result in depurination, base pair protonation, adenine, uracil, and cytosine unstacking and thus degradation of RNA [111]. The described changes found for low pH values can explain the CD profile found for the pH under study.

Polyplexes characterization

In order to determine the optimal complexation conditions, it was necessary to evaluate the degree of binding between sRNA and polycation at different N/P ratios. The polycations were mixed with sRNA for the formation of sRNA-polycation particles (polyplexes) in acetate buffer at pH 4.5 [64]. The pH 4.5 value was chosen because it is located within the range of pH values (4-6) that has been attributed to the endo/lysosomal compartment [38]. Moreover, at pH 4.5, the amine groups are to a large degree protonated and the cationic polyelectrolyte interacts with the negatively charged sRNA. We recall that the polycations possess pKa values (Table 2) higher than those of the phosphate groups of the RNA (pKa = 1.5) [90].

Table 2 – Main characteristics of L-PEI, B-PEI, CS-LMW, CS-MMW and PAA.

Polymer	*Molecular weight (MW)*[1]	*Monomer charge density*	*Nominal DD*[1] *(%)*	*Determined DD*[2] *(%)*	*pKa [ref]*
L-PEI	1300	11^+	-	-	9.26 [68]
B-PEI	10000	3^+	-	-	8.5 [112]
CS-LMW	50000 – 190000	1^+	75 – 85	83.14 ± 0.39	6.5 [68]
CS-MMW	190000 – 310000	1^+	75 – 85	73.86 ± 0.61	6.5 [68]
PAA	17000	1^+	-	-	8.5 [113]

[1] Provided by the manufacturer

[2] Determined by 1DUVS. The data represent the mean and standard error of at least three separate measurements (mean ± SD).

The influence of the formulation on the stability of the particles was examined by agarose electrophoresis (Figures 9-13). This technique detects nucleic acids, due to the presence of ethidium bromide/GelStar, as an intercaling agent with fluorescence, enabling the visualization of sRNA when the gel is exposed to UV radiation. In case the particles are sufficiently stable, sRNA molecules cannot spread out of the particles, and thus bands are not detected in the electrophoretic gel, i.e., the polyplexes are retained in the wells (neutralized sRNA). Otherwise, when particles are unstable, the electrophoretic voltage is sufficient to remove sRNA out of the particles and to induce their migration along the electrophoretic gel. Thus, the migration of sRNA is delayed depending on complexes stability. In preliminary studies, N/P ratio values among 0.625 to 50 were studied for all the selected polycation (L-PEI, B-PEI, CS-LMW, CS-MMW and PAA). sRNA molecules in the prepared particles interacted with all studied polycation, even at higher ratios of polycation/sRNA complexes (Figures 9-13). In this range, an intermediate region was found for each polycation, where most of the sRNA molecules are partially condensed, followed by complete condensation of the sRNA for large concentrations of polycation. Moreover, we have been studying different regions of condensation obtained for each polycation in more detail. It becomes therefore clear that the formation of stable nanoparticles occurs only at precise conditions as can be observed in Figures 9-13. For L-PEI (Figure 9), the bands corresponding to free sRNA in the L-PEI/sRNA complex were not observed when the polymer was present at N/P ratio above 3, whereas when the N/P ratios were 1.5 to 3, bands corresponding to free sRNA were observed (Figure 9).

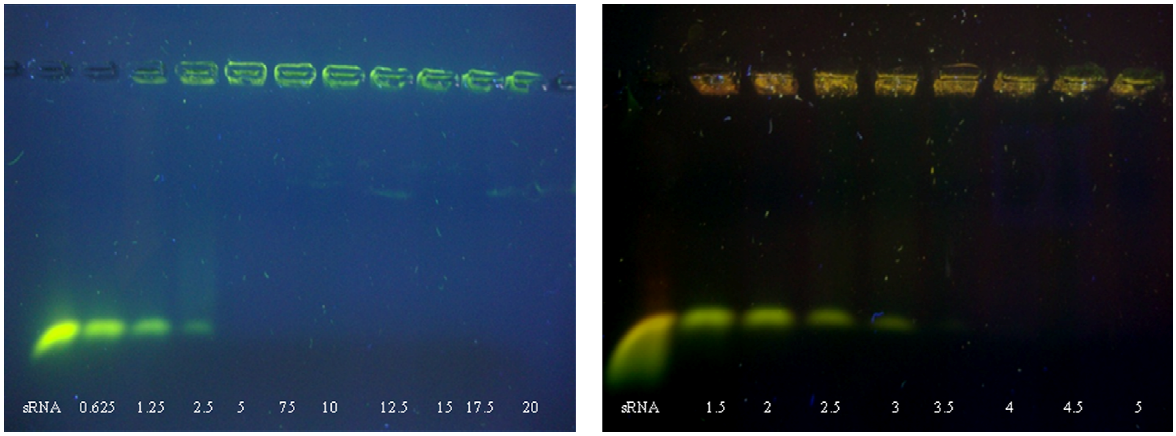

Figure 9 – Binding efficiency of sRNA/L-PEI polyplexes at various N/P ratios. The first lane of the gel corresponds to naked sRNA only. The numbers in each lane indicate the N/P ratios.

In the case of the B-PEI/sRNA complex, no suppression in the electrophoretic migration of sRNA was identified in complexes formed with N/P ratios of 1.25 to 2.5, while sRNA migration in complexes with N/P ratios higher than 2.5 was suppressed (Figure 10).

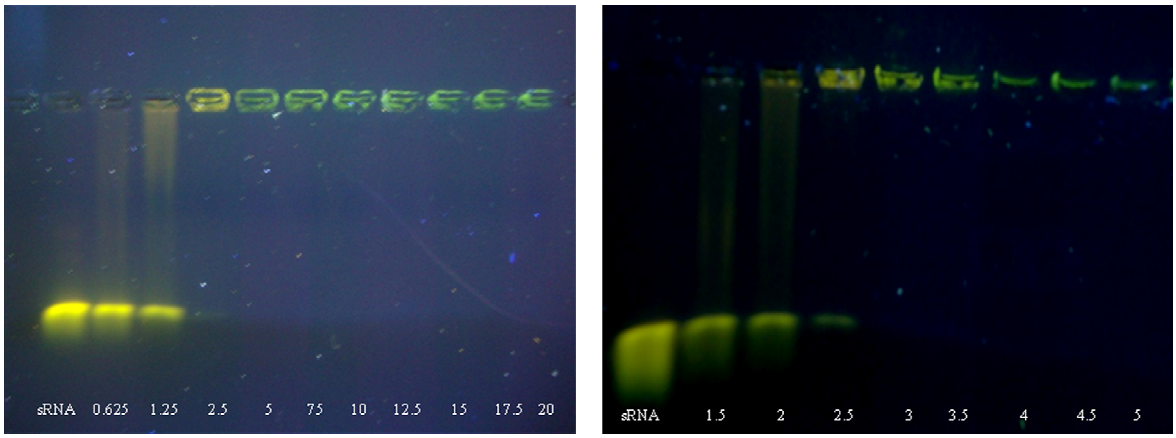

Figure 10 – Binding efficiency of sRNA/B-PEI polyplexes at various N/P ratios. The first lane of the gel corresponds to naked sRNA only. The numbers in each lane indicate the N/P ratios.

In comparison, the two PEIs in study display subtle differences in what concerns sRNA condensation. Lower concentration of B-PEI is required for full sRNA condensation. This result is in accordance with literature, where the binding constant between negative polyelectrolyte

and polycation has been shown to be dependent upon the valence of ligand [65, 114-116]. These results can be explained in terms of charge density and number of chains. L-PEI is a 1300 Da, linear polycation that contains mainly a secondary amine group and has a pKa of 9.38 [68]. B-PEI is slightly larger with 10 KDa, but it is branched and consists of primary, secondary and tertiary amine groups, which pKa of 8.5 [112]. Primary amines of PEI are reported to participate in forming complexes with nucleic acids, while secondary and tertiary amines are responsible for substantial endosomal disruption after endocytosis, due to their buffering effect at pHs under physiological conditions [2, 117]. The branched structure may promote a more efficient interaction with sRNA, as compared with to L-PEI, which may be beneficial for packaging. Note that sRNA possesses rigid structure [118, 119]. As such, branched, flexible, positive polymers appear to be suited for sRNA packing and delivery.

The characteristics of the different commercial chitosan (CS-LMW and CS-MMW) used in this work are shown in Table 2. MW and DD are the molecular weight and the deacetylation degree, respectively. The DD values represent the percentage of deacetylated primary amine groups along the molecular chain, which subsequently determines the positive charge density when chitosan is dissolved in acidic conditions (pH $\sim$ 5.5) [91]. Higher DD results in increased positive charge enabling a greater siRNA binding capacity [64]. Besides, the DD of chitosan influences the particle size and other characteristics like its encapsulation efficiency, an issue that will be further discussed. The CS-LMW complexes at an N/P ratio of 15 to 25, migrated into the gel, indicating the presence of uncomplexed sRNA. For higher N/P ratios, 30 to 50, the presence of polyplexes in the wells (neutralized sRNA) is observed, suggesting the sRNA is fully complexed at these N/P ratios (Figure 11). These N/P ratios values are in agreement with studies published for chitosan [79, 120]. The shorter length of siRNA as well as its rigid linearity can be expected to contribute to the weak interaction with CS, therefore, it is not surprising that it would need much higher density of CS to catch the protonated amine in the CS backbone and initiate complex formation [120]. These results can be explained in terms of charge density, because the CS contains low a spatial density charge, as compared with to L-PEI and B-PEI.

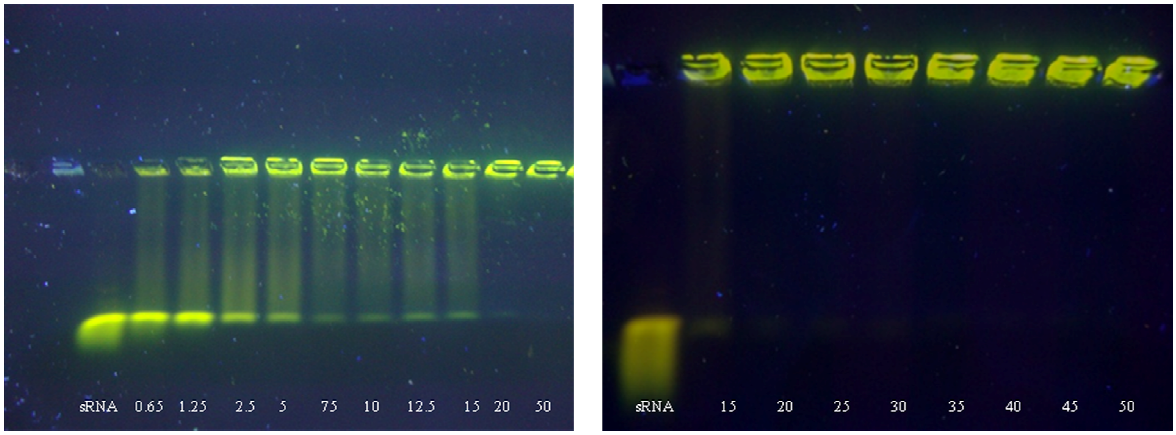

Figure 11 – Binding efficiency of sRNA/CS-LMW polyplexes at various N/P ratios. The first lane of the gel corresponds to naked sRNA only. The numbers in each lane indicate the N/P ratios.

The CS-MMW complexes at N/P ratios of 15 to 40, also migrated into the gel, but in samples prepared with N/P ratios of 40 or higher, it was not verified the migration of free sRNA (Figure 12).

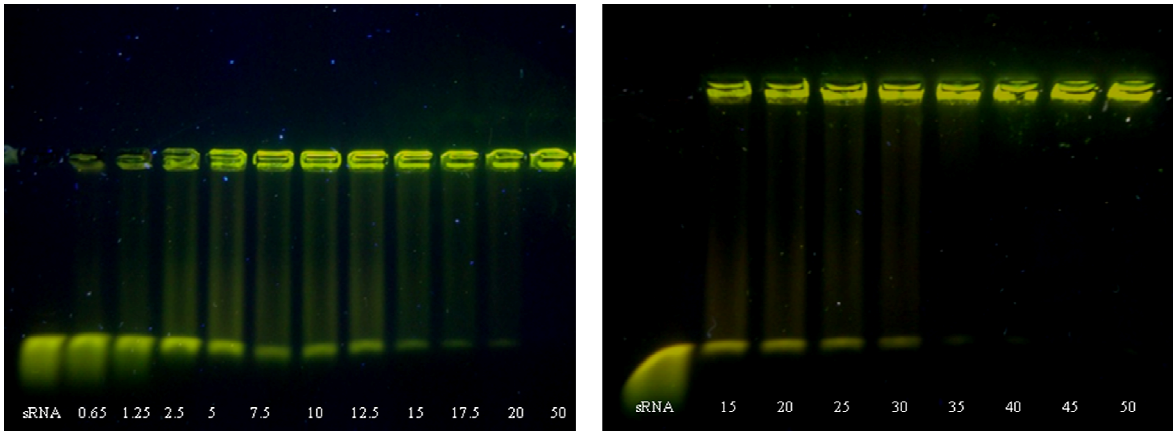

Figure 12 – Binding efficiency of sRNA/CS-MMW polyplexes at various N/P ratios. The first lane of the gel corresponds to naked sRNA only. The numbers in each lane indicate the N/P ratios.

This result depicts that some positively charged sRNA/CS-MMW complexes are present in solution. These observations seem to be contradictory to what is usually accepted, because a longer polycation chain usually promotes a larger sRNA compaction. However, the DD of the CS-LMW obtained was above 83 %, and that obtained for the CS-MMW was 73 % (Table 2). The CS-LMW possesses a higher cationic charge density than CS-MMW and is, consequently, more efficient in sRNA condensation. In this way, there is a more uniform distribution of the CS

charge on the sRNA molecule, which may explain the greater efficacy in inducing the condensation of sRNA, as observed in gel electrophoresis at low N/P ratios for CS-LMW (Figure 11 and 12). In agreement with these results, Kiang et al. (2004), previously reported that the degree of deacetylation affects the DNA binding [121]. Kiang et al. [121] have shown that the degree of chitosan deacetylation affects RNA binding, release and gene transfection efficiency *in vitro* and *in vivo*. We also have obtained the overcharged complexes for the CS-MMW/sRNA complexes, mainly at N/P ratios of 15 to 50 (Figure 12), since the process of formation of the complexes used in this study was the same. The overcharging process of a complex is not fully understood. It was clear that the polyanion-polycation complex formation and structure is ruled by a delicate balance between number of chains and their charge density. It is reasonable to assume that the overcharging process will be equally sensitive to such parameters. That is, it not clear which will have a larger impact in the formation of an overcharged complex, the charge density of the chain or their number [122].

In the case of the polycation PAA, sRNA complexation starts at very low N/P ratio values, as seen by the shift of the band and the presence of sRNA in the wells. More visible condensation starts at around N/P = 0.6 and at N/P = 0.8 where most sRNA molecules are complexed, as attested by the drastic decrease in intensity of the band that corresponds to free sRNA (Figure 13).

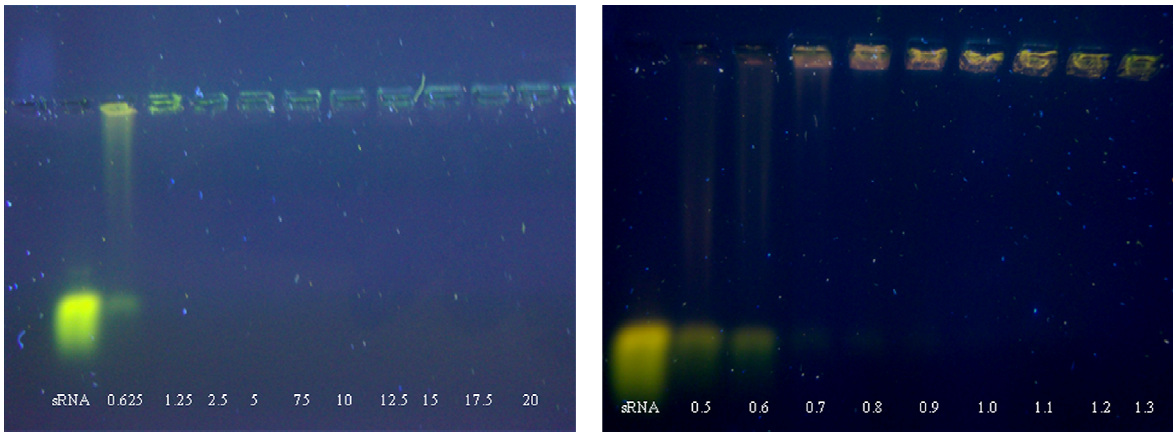

Figure 13 – Binding efficiency of sRNA/PAA polyplexes at various N/P ratios. The first lane of the gel corresponds to naked sRNA only. The numbers in each lane indicate the N/P ratios.

In this case, a smaller concentration of polycations is needed to induce the condensation of sRNA with PAA. This is not surprising because PAA is a polycation with a higher charge density and long chain, therefore promoting a stronger binding to sRNA.

Nanoparticle encapsulation efficiency

The ability of the carrier system to encapsulate as much genetic material as possible is an important parameter to improve the delivery of the sRNA to the cells. Hence, the sRNA loading efficiency was then determined spectrophotometrically by measuring the optical density of the supernatant obtained after centrifugation of nanoparticles (Figure 14). The results show that the amount of sRNA entrapped inside the polyplexes increases with the N/P ratio, suggesting that the encapsulation of sRNA is directly affect by the polymer charge available to interact with the negatively charged phosphate groups present in the sRNA backbone.

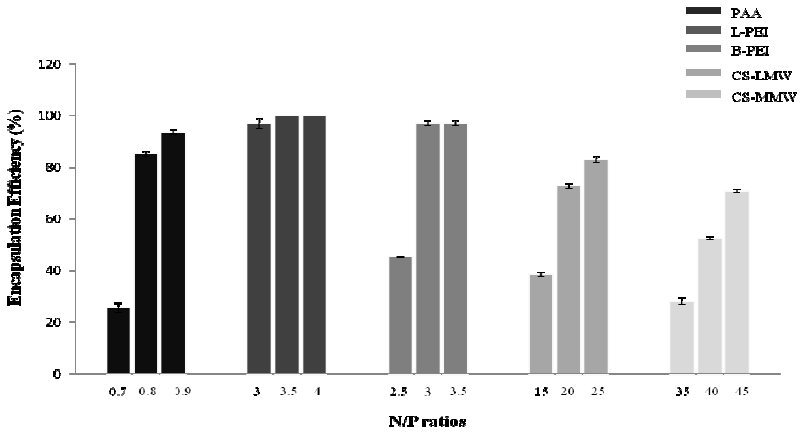

Figure 14- Encapsulation efficiency of the polyplexes obtained from different polymers. The data presents the average of three independent experiments. Bars in figure indicate standard deviation.

In accordance with the results obtained from the electrophoresis (Figure 9), 100 % of sRNA loading efficiency was achieved at the N/P ratio in the 3 to 4 region and at this point, sRNA was completely bound to the L-PEI/sRNA nanoparticles (Figure 14). The encapsulation studies of the B-PEI/sRNA complexes are consistent with the results of electrophoresis (Figure 10), in which we obtained 97 % of sRNA loading efficiency, for the 3 to 3.5 region (Figure 14). As the results in Figure 14 indicate, the encapsulation efficiency of the CS-LMW (%DD = 83.14) polyplexes is higher than that of the polyplexes synthesized with CS-MMW (%DD = 73.86). The results obtained for PAA/sRNA nanoparticles are in agreement with the results obtained from agarose gel electrophoresis, where a 25.6 % of sRNA loading efficiency was achieved at the N/P ratio of 0.7 and the highest N/P ratios was 85 % for an N/P ratio of 0.8 (Figure 14). Regarding the results for encapsulation efficiency in PAA samples, it is important to denote

that sRNA is more entrapped in these systems for small values of N/P ratios compared with the results obtained for the encapsulation of L-PEI and B-PEI with N/P ratios above, possibly due to the high linear charge density (which is a function of the polymer high molecular weight). PAA have a higher density of the amine groups that are loaded at the pH=4.5 used to promote the formation of polyplexes. In addition, as it will be shown in the study of PAA/sRNA size, it is the smallest particle used therefore, its sedimentation can be more difficult with the centrifugation time used. This fact could influence the precipitation ratio which can interfere in the method to determine encapsulation efficiency. Comparing the results obtained with the different polycations, we can suggest that the most suitable is L-PEI, since it is able to internalize higher sRNA quantities. These results entail the need for a compromise between the size of the carrier system and its ability to encapsulate the genetic material.

Polyplexes physicochemical properties

Zeta potential measurement provides vital information about the surface charge present on the nanoparticles. Although sRNA activity occurs in the cytoplasm, the delivery of sRNA faces many of the same challenges as gene delivery with polycationic complexes, from cell targeting to internalization and endosomal escape. The details of particle zeta potential and size of nanoparticles results are shown in Table 3, 4 and 5. In general, an evolution in the charge of the complexes towards positive (or more positive) values is observed for all systems in study, upon the addition of polymers (Table 3, 4 and 5). The trend is due to an increase in the number of positive charges, which counteract the negatively charged sRNA, present in a constant concentration. On the other hand, the size of the complexes should be in the range of 50 nm to 200 nm for efficient internalization by endocytic or other cell entry processes. Once inside the cell, they should dissociate to release the sRNA from the vector system to accomplish their respective functions [123-125]. So, the sizes corresponding to smaller polycation concentrations result from a mixture of sRNA-Polycation complexes and free sRNA molecules, and a reduction in size is seen when the polycation concentration increase, flowed by some expansion of the polyplexes at higher concentrations. The initial decrease in the sizes of the complexes is gradual, which is compatible with the gel electrophoresis observations (Figure 9-13). The net positive charge of the particles is desirable to prevent particle aggregation and promote electrostatic interaction with the overall negative charge of the cell membrane [79]. The L-PEI/sRNA complexes at the N/P ratios of 3, 3.5, 4 and 5 are positively charged nanoparticles with sizes ranging from 143.8 nm at a 3.5 ratio to 253.6 nm at a 2.5 ratio (Table 3). On the other hand, the B-PEI/sRNA complexes range from 144.3 nm at a 3 ratio to 371.2 nm at a 2.5 ratio. As expected, zeta potentials are negative for

complexes with N/P ratios lower than 2.5 and are positive for complexes with higher values (N/P ≥ 3). Hence, B-PEI/sRNA particles (+32.3 mV at a 3 ratio) were slightly more positively charged than those formulated with L-PEI (+11.7 mV at a 3 ratio) (Table 3).

Table 3 - Average zeta potential and size at various N/P ratios of sRNA and Polycation (L-PEI and B-PEI). All values are the mean ± SD of three independent experiments.

N/P ratio	Polyethyleneimine Linear		Polyethyleneimine Branched	
	Zeta potential ± SD (mV)	Size ± SD (nm)	Zeta potential ± SD (mV)	Size ± SD (nm)
2.5	-10.9 ± 0.6	253.6 ± 21.5	-3.4 ± 0.4	371.2 ± 18.4
3	11.7 ± 1.2	197.8 ± 11.2	32.3 ± 1.7	144.3 ± 1.5
3.5	19.4 ± 0.7	143.8 ± 6.9	32.0 ± 1.0	154.3 ± 1.9
4	20.6 ± 1.2	171.2 ± 1.2	29.9 ± 2.0	168.2 ± 0.9
5	24.3 ± 1.3	232 ± 1.7	26.6 ± 1.9	264.9 ± 2.3

sRNA/CS-LMW particles ranges in size from 156.5 nm (N/P = 30) to 237.5 nm (N/P = 40), and CS-MMW complexes ranged from 172.3 nm (N/P = 40) to 298.2 nm (N/P = 15) (Table 4). In addition, sRNA/CS-MMW particles display a smaller particle size with increasing N/P ratios, whereas the CS-LMW complexes size is almost constant in the range 20 at 35. A general trend that showed a decrease in the size of the complexes as the molecular weight of the chitosan decreased was also observed (Table 4). Although it may be expected that a medium molecular weight chitosan could interact with sRNA, and thus condense it more efficiently than a chitosan of a lower molecular weight. The results show that for both the used chitosans, the sizes of the complexes are comparable, however for CS-LMW (high DD) the sRNA condensation occurs for lower N/P ratio Table 4. The positive value of surface charge of the CS/sRNA complexes increases with increasing concentration of chitosan at a constant sRNA concentration, for N/P ratios greater than 15. Although sRNA/CS-LMW particles were slightly more positive than those formulated with CS-MMW (Table 4) this finding can be attributed to the fact that CS-MMW has a lower DD when compared to that of CS-LMW.

Table 4 – Average zeta potential and size at various N/P ratios of sRNA and Polycation (CS-LMW and CS-MMW). All values are the mean ± SD of three independent experiments.

N/P ratio	Chitosan-LMW		Chitosan-MMW	
	Zeta potential ± SD (mV)	Size ± SD (nm)	Zeta potential ± SD (mV)	Size ± SD (nm)
15	27.9 ± 0.7	215.0 ± 5.0	23.0 ± 0.2	298.2 ± 4.3
20	29.1 ± 0.4	157.6 ± 5.2	25.9 ± 0.4	242.9 ± 10.8
30	26.5 ± 1.0	156.5 ± 7.4	27.3 ± 0.9	193.2 ± 2.4
35	28.7 ± 0.9	182.2 ± 10.0	28.4 ± 0.4	172.3 ± 4.0
40	27.9 ± 1.1	237.4 ± 19.9	28.5 ± 0.6	177.7 ± 1.0

The PAA complexes at 0.6, 0.7, 0.8 and 0.9 N/P ratios are bellow 150 nm in diameter, which is considered the size limit for nonspecific endocytosis via clathrin-coated pits [116]. Concentration of PAA in nanoparticles also influences the surface charge of nanoparticles. As the concentration of PAA is increased, a higher zeta potential value is observed for the nanoparticles. At N/P ratios below 0.7, nanoparticles are negatively charged, since the system is deficient in polycation and sRNA molecules are not completely neutralized (Table 5). Results from the zeta potential measurements seem not to agree with those obtained in the encapsulation and the gel electrophoresis assays, since the compression range shifted to higher ratios. Two factors can contribute to this: (i) gel electrophoresis is expected to have a higher sensitivity to RNA detection, and (ii) the agarose gel is submersed in a buffer with pH 8.2, which can explain the shift to larger values of ratios, because at pH 8.2, the acetate buffers (pH = 4.5) are no longer effective.

Table 5 – Average zeta potential and size at various N/P ratios of sRNA and Polycation PAA. All values are the mean ± SD of three independent experiments.

N/P ratios	Poly(allylamine)	
	Zeta potential ± SD (mV)	Size ± SD (nm)
0.5	-13.5 ± 0.9	181.9 ± 5.7
0.6	-8.08 ± 2.5	98.3 ± 15.8
0.7	1.34 ± 0.3	86.4 ± 10.9
0.8	16.83 ± 1.8	115.8 ± 7.1
0.9	25.2 ± 0.4	121.9 ± 4.9

Morphology of polyplexes

In order to determine the morphology and the relative size of particles prepared with the different polycations, SEM technique was used to directly inspect the samples. Independently of the molecular weight, nanoparticles showed a very well defined spherical morphology and an uniform appearance (Figure 15A-E). However, there is discrepancy in sizes, relative to the previous PCS measurements, that probably a reflection of the different methods used. PCS was performed on nanoparticles in a fully hydrated state in solution, whereas SEM studies on dried samples. In addition, the PCS measurements present an average size range, whereas in SEM the sample size is small. For this reason, the use of different but complementary methods, allows an overall evaluation to be made of both size and morphology.

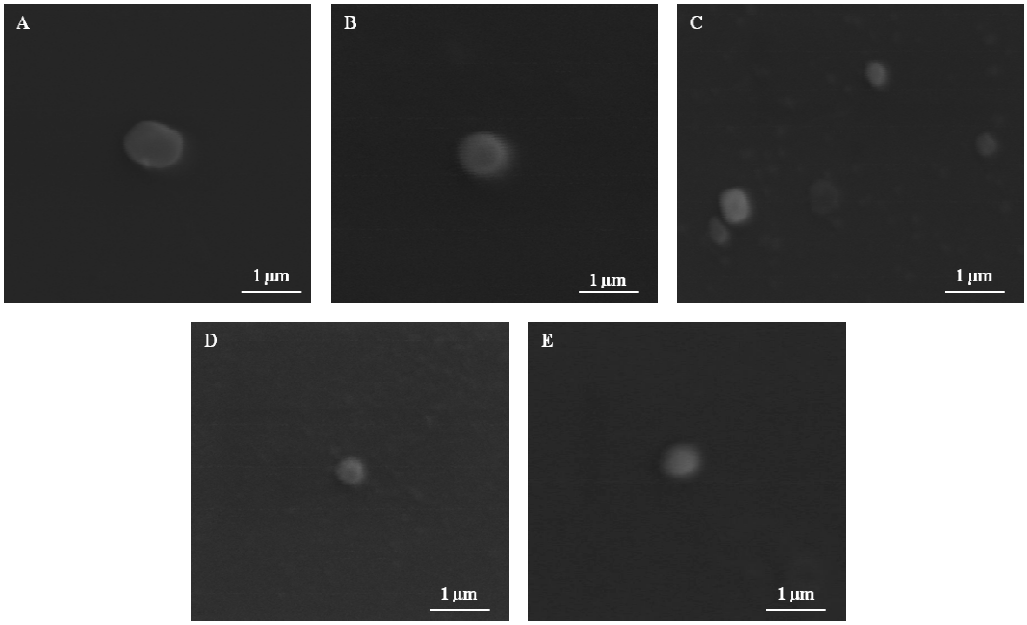

Figure 15 - Polyplexes obtained by simple complexation at pH 4.5 from commercial polymer and sRNA visualized by SEM. (A) sRNA/L-PEI (N/P = 3.5), (B) sRNA/B-PEI (N/P = 4), (C) sRNA/CS-LMW (N/P = 35), (D) sRNA/CS-MMW (N/P = 45) and (E) sRNA/PAA (N/P = 0.6). Scale bar, 1 µm.

Stability of polyplexes

The development of nanoparticles that are stable in the extracellular environment is essential for the protection of the genetic material. The polyplexes that survive in the blood stream should be subsequently delivered to the target cells without loss of RNA integrity. Thereby, serum nucleases are a major concern that affects RNA stability and consequently its transfection efficiency [70]. RNA must be stable to digestion by nuclease to have maximal activity in the cells [79]. In this way, to address if an appropriate protection of sRNA was promoted by its encapsulation, a stability studies with the polyplexes were performed using RNase and FBS. The results obtained are shown in Figures 16 and 17. The polyplexes were prepared as mentioned in Section II, at N/P ratios of 4.0; 4.5 and 5 with PEIs, 40; 45 and 50 with CSs and 1.1; 1.2 and 1.3 with PAA, and ressuspended in the PBS buffer with pH of 7.4. The polyplexes were incubated with 10 and 100 µg/mL concentrations of RNase over a period of 30 and 60 min at 37 ºC (Figure 16A-C).

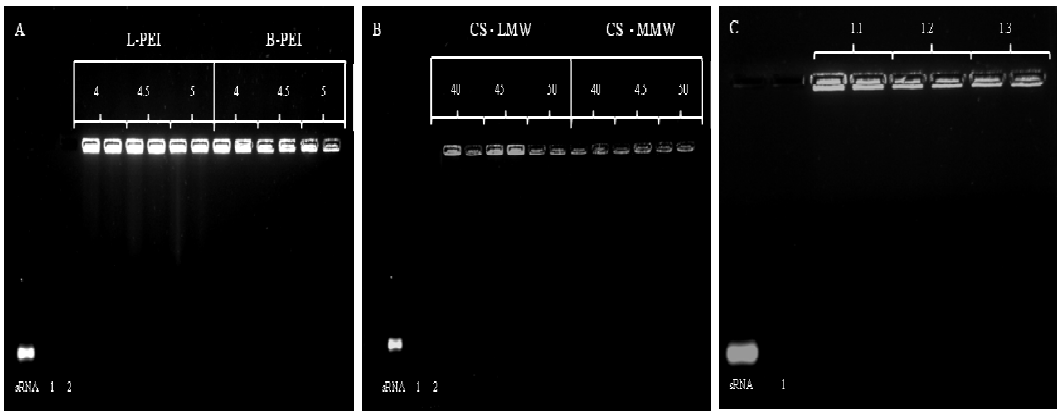

Figure 16 - Agarose gel electrophoresis of the nanoparticle following incubation with RNase (10 and 100 µg/mL) for 1h at 37 °C. (A) sRNA/L-PEI and sRNA/B-PEI, (B) sRNA/CS-LMW and sRNA/CS-MMW and (C) sRNA/PAA. Lane 1 – sRNA + RNAse (10 µg/mL) and Lane 2 – sRNA + RNAse (100 µg/mL).

In the case of L-PEI polyplexes, RNA degradation was observed at a 10 and 100 µg/mL enzyme concentration, for all N/P ratios studied (Figure 16A, lane 3 to 8). Regarding the protection promoted from the nanoparticulated systems, it should be noted that neither the sRNA in the polyplexes produced with CS nor PAA showed any signs of degradation when in contact with RNase (Figure 16B-C). Therefore, the structure of sRNA seems to be complexed more loosely in L-PEI polyplexes and hence RNase partially degrades the sRNA in the two enzyme concentrations, whereas B-PEI, CSs and PAA provide a complete protection (Figure

16A-C). Whereas the naked sRNA was completely degraded after 60 min of incubation (Figure 17, lane 1 and 2, respectively). Similar results are obtained when the polyplexes are incubated with 10 % of FBS at 37 ºC for 30 and 60 min (Figure 17A-C). As shown in Figure 17A, the degraded sRNA was visualized by the appearance of the sRNA bands in the lanes 3 to 8 of the L-PEI/sRNA complexes. On the other hand, sRNA complexed with the other polymers (B-PEI, CS-LMW, CS-MMW and PAA) do not indicate any signs of degradation, even after incubating with 10 % FBS for 1 h at 37 ºC, whereas the free sRNA rapidly degraded after 30 min of incubation at 37 ºC, as shown by the complete absence of sRNA bands in the gel in lanes 1. These results indicate that the serum nucleases are responsible for sRNA degradation as shown in lane 2 of the FBS gel (Figure 17A-C, lane 2). In general, these results revealed that B-PEI, CS-LMW, CS-MMW and PAA nanoparticles are able to protect sRNA from nuclease degradation (Figure 17A – lanes 9 to 15; B and C), suggesting that they are suitable delivery vehicles for *in vitro* and *in vivo* gene delivery applications.

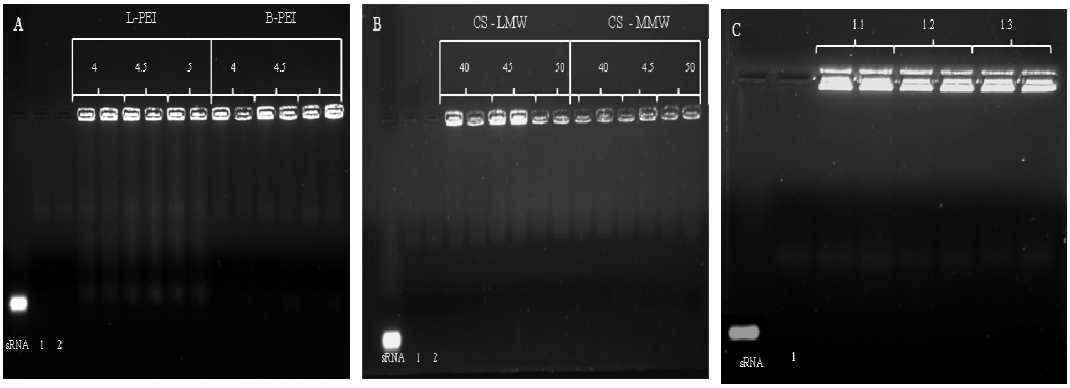

Figure 17- Agarose gel electrophoresis of the nanoparticle protection of sRNA following incubation with FBS for 30 min and 1h. (A) sRNA/L-PEI and sRNA/B-PEI, (B) sRNA/CS-LMW and sRNA/CS-MMW and (C) sRNA/PAA. Lane 1 – FBS (10%); Lane 2 – sRNA + FBS (10%).

The sulfated glycosaminoglycans and proteoglycans are the major constituents in the extracellular matrix of many tissues, but are also found inside and on the cell surface. Therefore, these mucopolisacharides are another possible limiting barrier for polyplexes in the access to target cells, since they may interact with the polyplexes having positively charged surfaces, which may affect the electrostatic forces that maintain the integrity of the particles and the mobility of the polyplexes in the tissue extracellular matrix [126, 127]. Therefore it is important to address the stability of the sRNA complexes in competing electrostatic conditions in the presence of negatively charged species such as heparin. In this

study heparin was chosen. Heparin is a polysaccharide negatively charged bearing sulfonate groups that competes with the nucleic acids, leading to dissociation. For this purpose, polyplexes are incubated with varying amounts of heparin (0.01, 0.1 and 0.5 IU/mL) to induce the decomplexation of the sRNA within the complexes, prior to separation on agarose gels (Figure 18A-E).

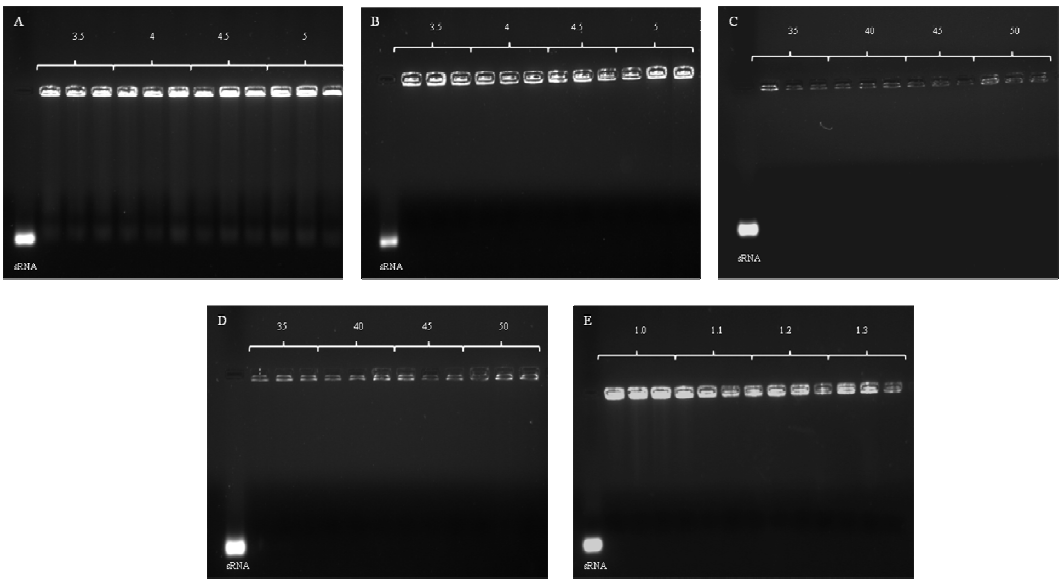

Figure 18 - Agarose gel electrophoresis of the nanoparticle following incubation with Heparin (0.01, 0.1 and 0.5 µg/mL) for 1h at 37 °C. (A) sRNA/L-PEI, (B) sRNA/B-PEI, (C) sRNA/CS-LMW, (D) sRNA/CS-MMW, (E) sRNA/PAA. Lane 1 – sRNA + Heparin (0.1 µg/mL) and Lane 2 – sRNA + Heparin (0.5 µg/mL).

All the L-PEI/sRNA complexes are unstable in the presence of heparin (Figure 18A). The results indicate that B-PEI/sRNA complexes are more stable than L-PEI/sRNA complexes at all charge ratios in the presence of heparin. (Figure 18A-B). The results obtained are in accordance with Kwok et al. (2010) [128]. Furthermore, the sRNA maintained stable complexes with CS-LMW and CS-MMW even in the presence of different concentrations of heparin (Figure 18C-D). The PAA/sRNA complexes formulated at N/P ratio of 1.0 dissociate with even trace amounts of heparin, but for N/P ratio of 1.1 the dissociation is achieved with approximately 0.01 IU/mL, and for the other concentrations of heparin the complexes are stable (Figure 18E). The sRNA in the PAA polyplexes is not released from the complexes by adding heparin to higher N/P ratios (Figure 18E). Overall, the results concerning the incubation with heparin for a period of 1 h demonstrate that the B-PEI and CS complexes with sRNA are more resistant to the heparin challenge than L-PEI and PAA complexes, and it is

expect that they are more efficient in transposing the cell membrane than L-PEI and PAA complexes.

Overall, the polyplexes B-PEI, CS-LMW and CS-MMW were able to accomplish the entrapment and protection of the sRNA inside their matrix. However, the capacity to dissociate in the presence of heparin is an indicator of the potential of the complex to dissociate within the cell and release the nucleic acid content, while providing sufficient stability outside the cells to protect genetic material and preserve the size and integrity of the nanoparticle.

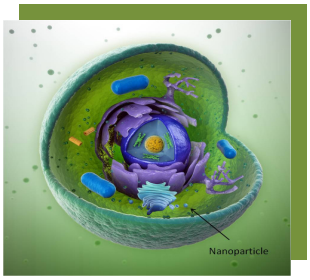

CHAPTER IV

Conclusions and Future Trends

The discovery of RNAi is highlighted by profound effect on studies of gene regulation, but also by the development of a new class of therapeutic agents based on small dsRNAs. The rapid progression from basic discovery to applications in medicine is unprecedented, and is indicative of the enormous therapeutic potential of RNAi. Generally, siRNA-based gene therapy applications rely on the use of synthetic siRNA. Although this process can be very efficient, the oligonucleotides typically presents contaminants, often referred to as failure sequences, which arise during synthesis. Therefore, the requirement for the production of highly purified and clinically suitable siRNA oligonucleotides arises as one of the most important challenge in the development of therapeutic strategies based on this technology, mostly because the presence of impurities may lead to non-targeted gene silencing, often associated with a decrease in therapeutic effectiveness. Thus, the recombinant production of biomolecules to be therapeutically applied is already well established. Hence, the purpose of this thesis was to develop and implement novel production methodologies for RNAi-based therapeutics. In addition, this thesis described the development of an integrative non-viral therapeutic strategy from production to application, since the delivery of these oligonucleotides into the cytoplasmic compartment, the location where their function is exerted, is usually a critical barrier to an efficient therapeutic response.

The use of *R. sulfidophilum* as an alternative host for sRNA production presents a number of advantages, since time-consuming RNA extraction and complex purification techniques are not necessary. This study contributes to the development of new procedures without the use of extremely toxic chemicals due to the absence of the host RNases. Therefore, it is purposed an improvement of process economics with high yields of sRNAs. Moreover, we have developed a strategy for *R. sulfidophilum* DSM 1374 growth using 3% NaCl at 30 ºC, which enables higher optical densities and an enhancement in sRNA production. Thus, according to the results obtained in this study, in order to obtain a high production of natural sRNA (maximum level of 197 ± 0.55 µg/mL) and minimizing impurities (gDNA, rRNA and proteins), *R. sulfidophilum* DSM 1374 should be cultivate up to 14 h. The successful recovery of sRNAs species with high yields in terms of quality and quantity is a step forward in RNA technology. These experiments with DSM 1374 showed relatively rapid growth and the highest production of the extracellular nucleic acids among the strains of *Rhodovulum* species tested by other authors. In conclusion, the bacterium study provides an alternative way for obtaining sRNAs with high yields. The successful results indicate an appropriate sRNA production, which makes

R. sulfidophilum a potential recombinant organism with large applicability in recombinant RNA therapeutics.

As it was referred above, it was necessary to develop a specialized delivery system that could transpose the innumerous cellular barriers to transfect and alongside protect and deliver the sRNA molecules to the cells. Thus, in this work it was also developed and characterized a group of nanoparticulated systems formulated with biocompatible different polymers. Their properties are highly dependent on structural parameters as weight, charge, structure and formulation (N/P ratio). In addition, their successful application, however, depends on optimizing physicochemical properties such as size, zeta potential, encapsulation efficiency and complex stability of the nanoparticles. The L-PEI/sRNA particles showed relatively small sizes and high encapsulation efficiency (100 %). However, they have low surface charges and are not stable in the presence of RNase, FBS or heparin. On the other hand, the B-PEI/sRNA promotes good encapsulation efficiency, presents small sizes and stability in the presence of RNase, FBS and heparin. In addition, it presents optimal values of zeta potential. The chitosan particles exhibit values the zeta potential that were always positive in the concentration ranges under study, sizes of about 200 nm and stability in the presence of RNase, FBS or heparin. However, they present low values of the encapsulation efficiency. Finally, the PAA/sRNA particles presented the smaller size, with good encapsulation efficiency and stability in mimetized physiological conditions. However, this particles display very low surface charges and PAA is known for its relatively high cytotoxicity. All the properties addressed in this work are highly dependent on structural parameters such as weight, charge, structure and formulation (N/P ratio). The N/P ratio seems a crucial factor, largely influencing particle size and the encapsulation of genetic material. These properties are often considered as important criteria to estimate the efficiency of the nanoparticle to deliver sRNA. The results presented here are a contribution for the optimization of properties of sRNA particles in therapeutic systems aiming at sRNA delivery.

From the conclusions drawn from this thesis also arise future perspectives to achieve an efficient and global strategy with a specific RNA. A recombinant production and application through delivery systems of a eukaryotic siRNA should be considered as an excellent approach for clinical application, since it can regulates gene expression by degrading mRNA with a high degree of specificity. Thus, the strategy to produce a siRNA target could be initiated by cloning the DNA sequence that produces the mature siRNA sequence into the pHSR1 vector. This vector has important features for siRNA production, such as the present of two ribozyme sequences flanking the target siRNA, which allows the recombinant siRNA release. The transformation of *R. sulfidophilum* host is then necessary to the optimization of siRNA production. The bacteria transformation could be performed either through electroporation or heat shock, because these techniques have not yet been described for *R. sulfidophilum*. The next step should include the purification/isolation of the target siRNA from the other host sRNAs. The development of an affinity-based methodology using amino acids as specific

ligands can be a potential approach for the RNA purification process, since this has been subject of study from our biotechnology group for the recent years, in addition to their successful results in DNA and RNA purification. Therefore, there is also the possibility to explore an affinity chromatographic technique for the development of new chromatographic ligands for siRNA. The development of a successful production and purification of siRNA would greatly benefit the subsequent condensation with polymers that are able of transposing the biological barriers and protect RNA from the deleterious action of RNases. Further *in vitro* studies would also be crucial to account for the capacity of the nanoparticles to target the intracellular compartment and promote gene silencing.

CHAPTER V

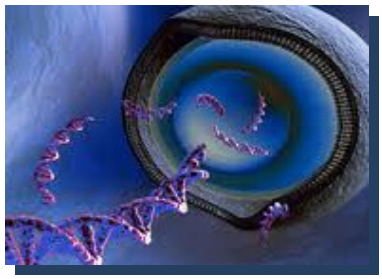

Bibliography

[1] Glover D, Lipps H, Jans D. Towards safe, non-viral therapeutic gene expression in humans. Nature Reviews Genetics 2005;6:299-310.

[2] Ahn CH, Chae SY, Bae YH, Kim SW. Biodegradable poly(ethylenimine) for plasmid DNA delivery. J Control Release 2002;80:273-282.

[3] El-Aneed A. An overview of current delivery systems in cancer gene therapy. J Control Release 2004;94:1-14.

[4] Morille M, Passirani C, Vonarbourg A, Clavreul A, Benoit J. Progress in developing cationic vectors for non-viral systemic gene therapy against cancer. Biomaterials 2008;29:3477-3496.

[5] Kim TH, Kim SI, Akaike T, Cho CS. Synergistic effect of poly(ethylenimine) on the transfection efficiency of galactosylated chitosan/DNA complexes. J Control Release 2005;105:354-366.

[6] Harris JD, Lemoine NR. Strategies for targeted gene therapy. Trends Genet 1996;12:400-405.

[7] Walton SP, Wu M, Gredell JA, Chan C. Designing highly active siRNAs for therapeutic applications. FEBS J 2010;277:4806-4813.

[8] Dessy A, Gorman JM. The emerging therapeutic role of RNA interference in disorders of the central nervous system. Clin Pharmacol Ther 2011;89:450-454.

[9] Qiao WL, Wang BC, Wang YZ, Yang LC, Zhang YQ, Shao PY. Cancer Therapy Based on Nanomaterials and Nanocarrier Systems. J Nanomater 2010;2010:9.

[10] Breaker RR. Natural and engineered nucleic acids as tools to explore biology. Nature 2004;432:838-845.

[11] Gong H, Liu CM, Liu DP, Liang CC. The role of small RNAs in human diseases: potential troublemaker and therapeutic tools. Med Res Rev 2005;25:361-381.

[12] Napoli C, Lemieux C, Jorgensen R. Introduction of a Chimeric Chalcone Synthase Gene into Petunia Results in Reversible Co-Suppression of Homologous Genes in trans. Plant Cell 1990;2:279-289.

[13] Fire A, Xu S, Montgomery MK, Kostas SA, Driver SE, Mello CC. Potent and specific genetic interference by double-stranded RNA in Caenorhabditis elegans. Nature 1998;391:806-811.

[14] Milhavet O, Gary DS, Mattson MP. RNA interference in biology and medicine. Pharmacol Rev 2003;55:629-648.

[15] Elbashir SM, Harborth J, Lendeckel W, Yalcin A, Weber K, Tuschl T. Duplexes of 21-nucleotide RNAs mediate RNA interference in cultured mammalian cells. Nature 2001;411:494-498.

[16] Yao YC, Wang CM, Varshney RR, Wang DA. Antisense Makes Sense in Engineered Regenerative Medicine. Pharm Res-Dord 2009;26:263-275.

[17] Takahashi Y, Nishikawa M, Takakura Y. Nonviral vector-mediated RNA interference: Its gene silencing characteristics and important factors to achieve RNAi-based gene therapy. Adv Drug Deliver Rev 2009;61:760-766.

[18] Tokatlian T, Segura T. siRNA applications in nanomedicine. Wires Nanomed Nanobi 2010;2:305-315.

[19] Dykxhoorn DM, Lieberman J. Running interference: prospects and obstacles to using small interfering RNAs as small molecule drugs. Annu Rev Biomed Eng 2006;8:377-402.

[20] Bernstein E, Caudy AA, Hammond SM, Hannon GJ. Role for a bidentate ribonuclease in the initiation step of RNA interference. Nature 2001;409:363-366.

[21] http://www.mellobiotech.com/page_b1.htm (6/11/2011).

[22] Chendrimada TP, Gregory RI, Kumaraswamy E, Norman J, Cooch N, Nishikura K, et al. TRBP recruits the Dicer complex to Ago2 for microRNA processing and gene silencing. Nature 2005;436:740-744.

[23] Gregory RI, Chendrimada TP, Cooch N, Shiekhattar R. Human RISC couples microRNA biogenesis and posttranscriptional gene silencing. Cell 2005;123:631-640.

[24] Kim DH, Rossi JJ. Strategies for silencing human disease using RNA interference. Nat Rev Genet 2007;8:173-184.

[25] Chiu YL, Ali A, Chu CY, Cao H, Rana TM. Visualizing a correlation between siRNA localization, cellular uptake, and RNAi in living cells. Chem Biol 2004;11:1165-1175.

[26] Morrissey DV, Lockridge J, Shaw L, Blanchard K, Jensen K, Breen W, et al. Potent and persistent in vivo anti-HBV activity of chemically modified siRNAs. Hepatology 2005;42:576a-576a.

[27] Akinc A, Zumbuehl A, Goldberg M, Leshchiner ES, Busini V, Hossain N, et al. A combinatorial library of lipid-like materials for delivery of RNAi therapeutics. Nat Biotechnol 2008;26:561-569.

[28] Wu SY, McMillan NA. Lipidic systems for in vivo siRNA delivery. AAPS J 2009;11:639-652.

[29] Peer D, Zhu P, Carman CV, Lieberman J, Shimaoka M. Selective gene silencing in activated leukocytes by targeting siRNAs to the integrin lymphocyte function-associated antigen-1. Proc Natl Acad Sci U S A 2007;104:4095-4100.

[30] Soutschek J, Akinc A, Bramlage B, Charisse K, Constien R, Donoghue M, et al. Therapeutic silencing of an endogenous gene by systemic administration of modified siRNAs. Nature 2004;432:173-178.

[31] Dassie JP, Liu XY, Thomas GS, Whitaker RM, Thiel KW, Stockdale KR, et al. Systemic administration of optimized aptamer-siRNA chimeras promotes regression of PSMA-expressing tumors. Nat Biotechnol 2009;27:839-849.

[32] Zabner J, Fasbender AJ, Moninger T, Poellinger KA, Welsh MJ. Cellular and Molecular Barriers to Gene-Transfer by a Cationic Lipid. J Biol Chem 1995;270:18997-19007.

[33] Gupta B, Levchenko TS, Torchilin VP. Intracellular delivery of large molecules and small particles by cell-penetrating proteins and peptides. Adv Drug Deliver Rev 2005;57:637-651.

[34] Parton RG, Simons K. The multiple faces of caveolae. Nat Rev Mol Cell Bio 2007;8:185-194.

[35] Petros RA, DeSimone JM. Strategies in the design of nanoparticles for therapeutic applications. Nat Rev Drug Discov 2010;9:615-627.

[36] Caracciolo G, Caminiti R, Digman MA, Gratton E, Sanchez S. Efficient Escape from Endosomes Determines the Superior Efficiency of Multicomponent Lipoplexes. Journal of Physical Chemistry B 2009;113:4995-4997.

[37] Varkouhi AK, Scholte M, Storm G, Haisma HJ. Endosomal escape pathways for delivery of biologicals. J Control Release 2011;151:220-228.

[38] Medina-Kauwe LK, Xie J, Hamm-Alvarez S. Intracellular trafficking of nonviral vectors. Gene Ther 2005;12:1734-1751.

[39] Dominska M, Dykxhoorn DM. Breaking down the barriers: siRNA delivery and endosome escape. J Cell Sci 2010;123:1183-1189.

[40] Nguyen DN, Green JJ, Chan JM, Longer R, Anderson DG. Polymeric Materials for Gene Delivery and DNA Vaccination. Adv Mater 2009;21:847-867.

[41] Suh J, Wirtz D, Hanes J. Efficient active transport of gene nanocarriers to the cell nucleus. Proc Natl Acad Sci U S A 2003;100:3878-3882.

[42] Obonyo O, Fisher E, Edwards M, Douroumis D. Quantum dots synthesis and biological applications as imaging and drug delivery systems. Crit Rev Biotechnol 2010;30:283-301.

[43] Hiraishi A, Ueda Y. Isolation and characterization of Rhodovulum strictum sp. nov. and some other purple nonsulfur bacteria from colored blooms in tidal and seawater pools. Int J Syst Bacteriol 1995;45:319-326.

[44] Hansen TA, Veldkamp H. Rhodopseudomonas sulfidophila, nov. spec., a new species of the purple nonsulfur bacteria. Arch Mikrobiol 1973;92:45-58.

[45] Hiraishi A, Ueda Y. Intrageneric Structure of the Genus Rhodobacter: Transfer of Rhodobacter sulfidophilus and Related Marine Species to the Genus Rhodovulum gen. nov. Int J Syst Bacteriol 1994;44:15-23.

[46] Watanabe M, Sasaki K, Nakashimada Y, Kakizono T, Noparatnaraporn N, Nishio N. Growth and flocculation of a marine photosynthetic bacterium Rhodovulum sp. Appl Microbiol Biot 1998;50:682-691.

[47] Watanabe M, Sasaki K, Nakashimada Y, Nishio N. High density cell culture of a marine photosynthetic bacterium Rhodovulum sc. with self-flocculated cells. Biotechnol Lett 1998;20:1113-1117.

[48] Havarstein LS, Coomaraswamy G, Morrison DA. An unmodified heptadecapeptide pheromone induces competence for genetic transformation in Streptococcus pneumoniae. Proc Natl Acad Sci U S A 1995;92:11140-11144.

[49] Steinmoen H, Knutsen E, Havarstein LS. Induction of natural competence in Streptococcus pneumoniae triggers lysis and DNA release from a subfraction of the cell population. Proc Natl Acad Sci U S A 2002;99:7681-7686.

[50] Whatmore AM, Barcus VA, Dowson CG. Genetic diversity of the streptococcal competence (com) gene locus. J Bacteriol 1999;181:3144-3154.

[51] Winzer K, Hardie KR, Williams P. Bacterial cell-to-cell communication: sorry, can't talk now - gone to lunch! Curr Opin Microbiol 2002;5:216-222.

[52] Ando T, Suzuki H, Nishimura S, Tanaka T, Hiraishi A, Kikuchi Y. Characterization of extracellular RNAs produced by the marine photosynthetic bacterium Rhodovulum sulfidophilum. J Biochem 2006;139:805-811.

[53] Suzuki H, Daimon M, Awano T, Umekage S, Tanaka T, Kikuchi Y. Characterization of extracellular DNA production and flocculation of the marine photosynthetic bacterium Rhodovulum sulfidophilum. Appl Microbiol Biotechnol 2009;84:349-356.

[54] Suzuki H, Umekage S, Tanaka T, Kikuchi Y. Extracellular tRNAs of the marine photosynthetic bacterium Rhodovulum sulfidophilum are not aminoacylated. Biosci Biotechnol Biochem 2009;73:425-427.

[55] Ando T, Suzuki H, Komura K, Tanaka T, Hiraishi A, Kikuchi Y. Extracellular RNAs produced by a marine photosynthetic bacterium Rhodovulum sulfidophilum. Nucleic Acids Symp Ser (Oxf) 2004:165-166.

[56] Suzuki H, Ando T, Umekage S, Tanaka T, Kikuchi Y. Extracellular production of an RNA aptamer by ribonuclease-free marine bacteria harboring engineered plasmids: a proposal for industrial RNA drug production. Appl Environ Microbiol 2010;76:786-793.

[57] Lee SY, Bailey SC, Apirion D. Small stable RNAs from Escherichia coli: evidence for the existence of new molecules and for a new ribonucleoprotein particle containing 6S RNA. J Bacteriol 1978;133:1015-1023.

[58] Wassarman KM, Zhang A, Storz G. Small RNAs in Escherichia coli. Trends Microbiol 1999;7:37-45.

[59] Windbichler N, von Pelchrzim F, Mayer O, Csaszar E, Schroeder R. Isolation of small RNA-binding proteins from E. coli: evidence for frequent interaction of RNAs with RNA polymerase. RNA Biol 2008;5:30-40.

[60] Nishimura S, Tanaka T, Fujita K, Itaya M, Hiraishi A, Kikuchi Y. Extracellular DNA and RNA produced by a marine photosynthetic bacterium Rhodovulum sulfidophilum. Nucleic Acids Res Suppl 2003:279-280.

[61] Hart SL. Multifunctional nanocomplexes for gene transfer and gene therapy. Cell Biol Toxicol 2010;26:69-81.

[62] Gao K, Huang L. Nonviral Methods for siRNA Delivery. Mol Pharmaceut 2009;6:651-658.

[63] Park TG, Jeong JH, Kim SW. Current status of polymeric gene delivery systems. Adv Drug Deliver Rev 2006;58:467-486.

[64] Dehousse V, Garbacki N, Jaspart S, Castagne D, Piel G, Colige A, et al. Comparison of chitosan/siRNA and trimethylchitosan/siRNA complexes behaviour in vitro. Int J Biol Macromol 2010;46:342-349.

[65] Nimesh S, Chandra R. Polyethylenimine nanoparticles as an efficient in vitro siRNA delivery system. Eur J Pharm Biopharm 2009;73:43-49.

[66] Cho K, Wang X, Nie S, Chen ZG, Shin DM. Therapeutic nanoparticles for drug delivery in cancer. Clin Cancer Res 2008;14:1310-1316.

[67] http://www.google.com/imgres?imgurl=http://img.medscape.com/article/740/169/740169-fig1.jpg&imgrefurl=http://www.medscape.com/viewarticle/740169_2&usg=__cnwA060nSqol-xBX1lKJdzlk7ZI=&h=625&w=796&sz=73&hl=en&start=685&zoom=1&tbnid=gxKT2JhZkeEYcM:&tbnh=165&tbnw=210&ei=_rrzTdjNEIbRtAa8jKWzBg&prev=/search%3Fq%3Dnanocarriers%26um%3D1%26hl%3Den%26rlz%3D1I7PRFA_pt-PT%26biw%3D1345%26bih%3D513%26tbm%3Disch&chk=sbg&um=1&itbs=1&iact=rc&dur=202&page=55&ndsp=12&ved=1t:429,r:1,s:685&tx=162&ty=56. (11/6/2011)

[68] De Smedt SC, Demeester J, Hennink WE. Cationic polymer based gene delivery systems. Pharm Res 2000;17:113-126.

[69] Gebhart CL, Kabanov AV. Evaluation of polyplexes as gene transfer agents. J Control Release 2001;73:401-416.

[70] Mao S, Sun W, Kissel T. Chitosan-based formulations for delivery of DNA and siRNA. Adv Drug Deliv Rev 2010;62:12-27.

[71] Elouahabi A, Ruysschaert JM. Formation and intracellular trafficking of lipoplexes and polyplexes. Mol Ther 2005;11:336-347.

[72] Howard KA. Delivery of RNA interference therapeutics using polycation-based nanoparticles. Adv Drug Deliver Rev 2009;61:710-720.

[73] Tros de Ilarduya C, Sun Y, Duzgunes N. Gene delivery by lipoplexes and polyplexes. Eur J Pharm Sci 2010;40:159-170.

[74] Mintzer MA, Simanek EE. Nonviral Vectors for Gene Delivery. Chem Rev 2009;109:259-302.

[75] Godbey WT, Wu KK, Mikos AG. Poly(ethylenimine) and its role in gene delivery. J Control Release 1999;60:149-160.

[76] Mao S, Sun W, Kissel T. Chitosan-based formulations for delivery of DNA and siRNA. Advanced Drug Delivery Reviews 2009.

[77] Rudzinski WE, Aminabhavi TM. Chitosan as a carrier for targeted delivery of small interfering RNA. Int J Pharm 2010;399:1-11.

[78] Borchard G. Chitosans for gene delivery. Advanced Drug Delivery Reviews 2001;52:145-150.

[79] Katas H, Alpar HO. Development and characterisation of chitosan nanoparticles for siRNA delivery. J Control Release 2006;115:216-225.

[80] Liu X, Howard KA, Dong M, Andersen MO, Rahbek UL, Johnsen MG, et al. The influence of polymeric properties on chitosan/siRNA nanoparticle formulation and gene silencing. Biomaterials 2007;28:1280-1288.

[81] Pathak A, Aggarwal A, Kurupati RK, Patnaik S, Swami A, Singh Y, et al. Engineered polyallylamine nanoparticles for efficient in vitro transfection. Pharm Res 2007;24:1427-1440.

[82] Alkilany AM, Nagaria PK, Hexel CR, Shaw TJ, Murphy CJ, Wyatt MD. Cellular uptake and cytotoxicity of gold nanorods: molecular origin of cytotoxicity and surface effects. Small 2009;5:701-708.

[83] Mawad D, Lauto A, Penciu A, Mehier H, Fenet B, Fessi H, et al. Synthesis and characterization of novel radiopaque poly(allyl amine) nanoparticles. Nanotechnology 2010;21:335603.

[84] Boussif O, Delair T, Brua C, Veron L, Pavirani A, Kolbe HV. Synthesis of polyallylamine derivatives and their use as gene transfer vectors in vitro. Bioconjug Chem 1999;10:877-883.

[85] Martins R, Queiroz JA, Sousa F. A new affinity approach to isolate Escherichia coli 6S RNA with histidine-chromatography. J Mol Recognit 2010;23:519-524.

[86] Sousa F, Prazeres DM, Queiroz JA. Improvement of transfection efficiency by using supercoiled plasmid DNA purified with arginine affinity chromatography. J Gene Med 2009;11:79-88.

[87] Laemmli UK. Cleavage of structural proteins during the assembly of the head of bacteriophage T4. Nature 1970;227:680-685.

[88] Chomczynski P, Sacchi N. The single-step method of RNA isolation by acid guanidinium thiocyanate-phenol-chloroform extraction: twenty-something years on. Nat Protoc 2006;1:581-585.

[89] Huh MS, Lee SY, Park S, Lee S, Chung H, Choi Y, et al. Tumor-homing glycol chitosan/polyethylenimine nanoparticles for the systemic delivery of siRNA in tumor-bearing mice. J Control Release 2010;144:134-143.

[90] Mel'nikova YSL, B. . pH-Controlled DNA Condensation in the Presence of Dodecyldimethylamine Oxide. Langmuir 2000;16:5871–5878.

[91] Tan SC, Khor E, Tan TK, Wong SM. The degree of deacetylation of chitosan: advocating the first derivative UV-spectrophotometry method of determination. Talanta 1998;45:713-719.

[92] Pecot CV, Calin GA, Coleman RL, Lopez-Berestein G, Sood AK. RNA interference in the clinic: challenges and future directions. Nat Rev Cancer 2011;11:59-67.

[93] Masuda S, Yoshida M, Nagashima KV, Shimada K, Matsuura K. A new cytochrome subunit bound to the photosynthetic reaction center in the purple bacterium, Rhodovulum sulfidophilum. J Biol Chem 1999;274:10795-10801.

[94] Appia-Ayme C, Little PJ, Matsumoto Y, Leech AP, Berks BC. Cytochrome complex essential for photosynthetic oxidation of both thiosulfate and sulfide in Rhodovulum sulfidophilum. J Bacteriol 2001;183:6107-6118.

[95] Kimura Y, Alric J, Vermeglio A, Masuda S, Hagiwara Y, Matsuura K, et al. A new membrane-bound cytochrome c works as an electron donor to the photosynthetic reaction center complex in the purple bacterium, Rhodovulum sulfidophilum. J Biol Chem 2007;282:6463-6472.

[96] Masuda S, Nagashima KV, Shimada K, Matsuura K. Transcriptional control of expression of genes for photosynthetic reaction center and light-harvesting proteins in the purple bacterium Rhodovulum sulfidophilum. J Bacteriol 2000;182:2778-2786.

[97] Imhoff JF. True marine and halophilic anoxygenic phototrophic bacteria. Arch Microbiol 2001;176:243-254.

[98] Watanabe M, Shiba H, Sasaki K, Nakashimada Y, Nishio N. Promotion of growth and flocculation of a marine photosynthetic bacterium, Rhodovulum sp. by metal cations. Biotechnol Lett 1998;20:1109-1112.

[99] Csonka LN. Physiological and genetic responses of bacteria to osmotic stress. Microbiol Rev 1989;53:121-147.

[100] Farrell RE. RNA Methodologies. York, USA: Academic Press; 2005.

[101] Madabusi LV, Latham GJ, Andruss BF. RNA extraction for arrays. Methods Enzymol 2006;411:1-14.

[102] Noparatnaraporn N, Watanabe M, Choorit W, Sasaki K. Production of RNA by a marine photosynthetic bacterium, Rhodovulum sp. Biotechnol Lett 2000;22:1867-1870.

[103] Chu CY, Rana TM. Small RNAs: regulators and guardians of the genome. J Cell Physiol 2007;213:412-419.

[104] Sambrook J, Fritsch EF, Maniatis T. Molecular cloning: a laboratory manual. New York: Cold Spring Harbor Laboratory Press; 2001.

[105] Gaspar VM, Sousa F, Queiroz JA, Correia IJ. Formulation of chitosan-TPP-pDNA nanocapsules for gene therapy applications. Nanotechnology 2011;22:015101.

[106] Conwell CC, Hud NV. Evidence that both kinetic and thermodynamic factors govern DNA toroid dimensions: effects of magnesium(II) on DNA condensation by hexammine cobalt(III). Biochemistry 2004;43:5380-5387.

[107] Conwell CC, Vilfan ID, Hud NV. Controlling the size of nanoscale toroidal DNA condensates with static curvature and ionic strength. Proc Natl Acad Sci U S A 2003;100:9296-9301.

[108] Sarkar T, Conwell CC, Harvey LC, Santai CT, Hud NV. Condensation of oligonucleotides assembled into nicked and gapped duplexes: potential structures for oligonucleotide delivery. Nucleic Acids Res 2005;33:143-151.

[109] Shovsky A, Varga I, Makuska R, Claesson PM. Formation and stability of water-soluble, molecular polyelectrolyte complexes: effects of charge density, mixing ratio, and polyelectrolyte concentration. Langmuir 2009;25:6113-6121.

[110] Ma PLL, M.; Winnik, F. M.; Buschmann, M. D. New Insights into Chitosan−DNA Interactions Using Isothermal Titration Microcalorimetry. Biomacromolecules 2009;10:1490-1499.

[111] Doty P, Boedtker H, Fresco JR, Haselkorn R, Litt M. Secondary Structure in Ribonucleic Acids. Proc Natl Acad Sci U S A 1959;45:482-499.

[112] Choosakoonkriang S, Lobo BA, Koe GS, Koe JG, Middaugh CR. Biophysical characterization of PEI/DNA complexes. J Pharm Sci 2003;92:1710-1722.

[113] Kini GC, Lai J, Wong MS, Biswal SL. Microfluidic formation of ionically cross-linked polyamine gels. Langmuir 2010;26:6650-6656.

[114] Jorge AF, Dias RS, Pereira JC, Pais AA. DNA condensation by pH-responsive polycations. Biomacromolecules 2010;11:2399-2406.

[115] Bonnet ME, Erbacher P, Bolcato-Bellemin AL. Systemic delivery of DNA or siRNA mediated by linear polyethylenimine (L-PEI) does not induce an inflammatory response. Pharm Res 2008;25:2972-2982.

[116] Grayson AC, Doody AM, Putnam D. Biophysical and structural characterization of polyethylenimine-mediated siRNA delivery in vitro. Pharm Res 2006;23:1868-1876.

[117] Demeneix B, Behr J, Boussif O, Zanta MA, Abdallah B, Remy J. Gene transfer with lipospermines and polyethylenimines. Adv Drug Deliv Rev 1998;30:85-95.

[118] Kebbekus P, Draper DE, Hagerman P. Persistence length of RNA. Biochemistry 1995;34:4354-4357.

[119] Hagerman PJ. Flexibility of RNA. Annu Rev Biophys Biomol Struct 1997;26:139-156.

[120] Techaarpornkul S, Wongkupasert S, Opanasopit P, Apirakaramwong A, Nunthanid J, Ruktanonchai U. Chitosan-mediated siRNA delivery in vitro: effect of polymer molecular weight, concentration and salt forms. AAPS PharmSciTech 2010;11:64-72.

[121] Kiang T, Wen J, Lim H, Leong K. The effect of the degree of chitosan deacetylation on the efficiency of gene transfection. Biomaterials 2004;25:5293-5301.

[122] Ravindran S, Wu J. Overcharging of nanoparticles in electrolyte solutions. Langmuir 2004;20:7333-7338.

[123] Gao H, Shi W, Freund LB. Mechanics of receptor-mediated endocytosis. Proc Natl Acad Sci U S A 2005;102:9469-9474.

[124] Aoki H, Satoh M, Mitsuzuka K, Ito A, Saito S, Funato T, et al. Inhibition of motility and invasiveness of renal cell carcinoma induced by short interfering RNA transfection of beta 1,4GalNAc transferase. FEBS Lett 2004;567:203-208.

[125] Gary DJ, Puri N, Won YY. Polymer-based siRNA delivery: perspectives on the fundamental and phenomenological distinctions from polymer-based DNA delivery. J Control Release 2007;121:64-73.

[126] Glodde M, Sirsi SR, Lutz GJ. Physiochemical properties of low and high molecular weight poly(ethylene glycol)-grafted poly(ethylene imine) copolymers and their complexes with oligonucleotides. Biomacromolecules 2006;7:347-356.

[127] Lee SY, Huh MS, Lee S, Lee SJ, Chung H, Park JH, et al. Stability and cellular uptake of polymerized siRNA (poly-siRNA)/polyethylenimine (PEI) complexes for efficient gene silencing. J Control Release 2010;141:339-346.

[128] Kwok A, Hart SL. Comparative structural and functional studies of nanoparticle formulations for DNA and siRNA delivery. Nanomedicine 2011;7:210-219.